Search for massive WH resonances decaying into the l nu b(b)over-bar final state at root s=8 TeV

Khachatryan, V.

2016-04-28

Khachatryan , V , Eerola , P , Pekkanen , J , Voutilainen , M , Härkönen , J , Karimäki , V , Kinnunen , R , Lampén , T , Lassila-Perini , K , Lehti , S , Lindén , T , Luukka , P , Mäenpää , T , Peltola , T , Tuominen , E , Tuominiemi , J , Tuovinen , E , Wendland , L , Talvitie , J , Tuuva , T & The CMS Collaboration 2016 , ' Search for massive WH resonances decaying into the l nu b(b)over-bar final state at root s=8 TeV ' , European Physical Journal C. Particles and Fields , vol. 76 , no. 5 , 237 . https://doi.org/10.1140/epjc/s10052-016-4067-z

http://hdl.handle.net/10138/164564
https://doi.org/10.1140/epjc/s10052-016-4067-z

unspecified
publishedVersion

Eur. Phys. J. C (2016) 76:237
DOI 10.1140/epjc/s10052-016-4067-z

THE EUROPEAN PHYSICAL JOURNAL C

Regular Article - Experimental Physics

Search for massive WH resonances decaying into the $\ell\nu b\bar{b}$ final state at $\sqrt{s} = 8$ TeV

CMS Collaboration*

CERN, 1211 Geneva 23, Switzerland

Received: 24 January 2016 / Accepted: 8 April 2016

Abstract A search for a massive resonance W′ decaying into a W and a Higgs boson in the $\ell\nu b\bar{b}$ (ℓ = e, μ) final state is presented. Results are based on data corresponding to an integrated luminosity of 19.7 fb^{-1} of proton–proton collisions at $\sqrt{s} = 8$ TeV, collected using the CMS detector at the LHC. For a high-mass ($\gtrsim$1 TeV) resonance, the two bottom quarks coming from the Higgs boson decay are reconstructed as a single jet, which can be tagged by placing requirements on its substructure and flavour. Exclusion limits at 95 % confidence level are set on the production cross section of a narrow resonance decaying into WH, as a function of its mass. In the context of a little Higgs model, a lower limit on the W′ mass of 1.4 TeV is set. In a heavy vector triplet model that mimics the properties of composite Higgs models, a lower limit on the W′ mass of 1.5 TeV is set. In the context of this model, the results are combined with related searches to obtain a lower limit on the W′ mass of 1.8 TeV, the most restrictive to date for decays to a pair of standard model bosons.

1 Introduction

This paper presents a search for massive resonances decaying into a W and a standard model (SM) Higgs boson (H) [1–4] in the $\ell\nu b\bar{b}$ (ℓ = e, μ) final state. Such processes are distinctive features of several extensions of the SM such as composite Higgs [5–7], SU(5)/SO(5) Littlest Higgs (LH) [8–11], technicolor [12,13], and left-right symmetric models [14]. These models provide solutions to the hierarchy problem and predict new particles including additional gauge bosons such as a heavy W′. The W′ in these models can have large branching fractions to WH and WZ, while the decays to fermions can be suppressed. The recently proposed heavy vector triplet (HVT) model [15] generalizes a large class of specific models that predict new heavy spin-1 vector bosons. In this model, the resonance is described by a simplified Lagrangian in terms of a small number of parameters representing its mass and couplings to SM bosons and fermions.

For a W′ with SM couplings to fermions and thus reduced decay branching ratio to SM bosons, the most stringent limits on production cross sections are reported in searches with leptonic final states [16,17]. The current lower limit on the W′ mass is 3.3 TeV. In the same context, searches for a W′ decaying into a pair of SM vector bosons (WZ) [18–21] provide a lower mass limit of 1.7 TeV. In the context of a HVT model with reduced couplings to fermions (HVT model B), the most stringent limit of 1.7 TeV on the W′/Z′ mass is set by a search for $W'/Z' \to WH/ZH \to q\bar{q}b\bar{b}$ [22]. The same model is used to interpret the results of a search for $W'/Z' \to WH/ZH \to \ell\nu/\ell\ell/\nu\nu + b\bar{b}$ [23]. A lower limit on the W′ mass of 1.5 TeV is set in the same final state reported in Ref. [23]. Finally, a specific search for $Z' \to ZH \to q\bar{q}\tau^+\tau^-$ was reported in Ref. [24] and interpreted in the context of the same HVT model B.

This analysis is based on proton–proton collision data at $\sqrt{s} = 8$ TeV collected by the CMS experiment at the CERN LHC during 2012, corresponding to an integrated luminosity of 19.7 fb^{-1}. The signal considered is the production of a resonance with mass above 0.8 TeV decaying into WH, where the Higgs boson decays into a bottom quark–antiquark pair and the W boson decays into a charged lepton and a neutrino (Fig. 1). It is assumed that the resonance is narrow, i.e. that its intrinsic width is much smaller than the experimental resolution.

The search strategy is closely related to the search for high mass WW resonances in the $\ell\nu q\bar{q}$ final state, described in Ref. [25], with the addition of b tagging techniques. We search for resonances in the invariant mass of the WH system on top of a smoothly falling background distribution, where the background mainly comprises events involving pair produced top quarks ($t\bar{t}$) or a W boson produced in association with jets (W+jets). For the resonance mass range considered, the two quarks from the Higgs boson decay would be separated by a small angle, resulting in the detection of a single jet after hadronization. This jet is tagged as coming from

* e-mail: cms-publication-committee-chair@cern.ch

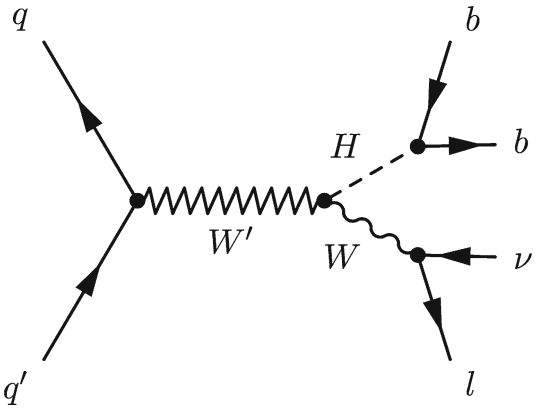

Fig. 1 Production of a resonance decaying into WH

a Higgs boson through the estimation of its invariant mass, application of jet substructure techniques [26], and use of specialized b tagging techniques for high transverse momentum (p_T) Higgs bosons [27].

The results of this analysis are also combined with two previous results [22,24] to obtain a further improvement in sensitivity.

2 CMS detector

The central feature of the CMS apparatus is a superconducting solenoid of 6 m internal diameter, providing a field of 3.8 T. Within the field volume are a silicon pixel and strip tracker, a crystal electromagnetic calorimeter (ECAL), and a brass and scintillator hadronic calorimeter (HCAL). The CMS tracker consists of 1440 silicon pixel and 15 148 silicon strip detector modules covering a pseudorapidity range of $|\eta| < 2.5$. The ECAL consists of nearly 76 000 lead tungstate crystals, which provide coverage of $|\eta| < 1.48$ in the central barrel region and $1.48 < |\eta| < 3.00$ in the two forward endcap regions. The HCAL consists of a sampling calorimeter [28], which utilizes alternating layers of brass as an absorber and plastic scintillator as an active material, covering the range $|\eta| < 3$, and is extended to $|\eta| < 5$ by a forward hadron calorimeter. Muons are measured in the range $|\eta| < 2.4$ with detection planes which employ three technologies: drift tubes, cathode strip chambers, and resistive-plate chambers. The muon trigger combines the information from the three sub-detectors with a coverage up to $|\eta| < 2.1$. A more detailed description of the CMS detector, together with a definition of the coordinate system used and the relevant kinematic variables, can be found in Ref. [28].

3 Simulated samples

For the modelling of the background we use the MADGRAPH v5.1.3.30 [29] event generator to simulate the production of W boson and Drell–Yan events in association with jets, the POWHEG 1.0 r1380 [30–35] package to generate $t\bar{t}$ and single top quark events, and PYTHIA v6.424 [36] for diboson (WW, WZ, and ZZ) processes. All simulated event samples are generated using the CTEQ6L1 [37] parton distribution functions (PDF) set, except for the POWHEG $t\bar{t}$ sample, for which the CT10 PDF set [38] is used. All the samples are then processed further by PYTHIA, using the Z2* tune [39,40] for simulation of parton showering and subsequent hadronization, and for simulation of the underlying event. The passage of the particles through the CMS detector is simulated using the GEANT4 package [41]. All simulated background samples are normalized to the integrated luminosity of the recorded data, using inclusive cross sections determined at next-to-leading order, or next-to-next-to-leading order when available, calculated with MCFM v6.6 [42–45] and FEWZ v3.1 [46], except for the $t\bar{t}$ sample, for which TOP++ v2.0 [47] is used.

To simulate the signature of interest, we use a model of a generic narrow spin-1 W′ resonance implemented with MADGRAPH. We verified that the kinematic distributions agree with those predicted by implementations of the LH, composite Higgs and HVT models in MADGRAPH. The resonance width differs in the three models, but in each case it is found to be negligible with respect to the experimental resolution. More details on the parameters used for interpretation of the models are given in Sect. 8.

Extra proton–proton interactions are combined with the generated events before detector simulation to match the observed distribution of the number of additional interactions per bunch crossing (pileup). The simulated samples are also corrected for observed differences between data and simulation in the efficiencies of the lepton trigger [16], the lepton identification/isolation [16], and the selection criteria identifying jets originating from hadronization of bottom quarks (b-tagged jets) [27].

4 Reconstruction and selection of events

4.1 Trigger and basic event selection

Candidate events are selected during data taking using single-lepton triggers, which require either one electron or one muon without isolation requirements. For electrons the minimum transverse momentum p_T measured at the high level trigger is 80 GeV, while for muons the p_T must be greater than 40 GeV.

After trigger selection, all events are required to have at least one primary-event vertex reconstructed within a 24 cm window along the beam axis, with a transverse distance from the nominal pp interaction region of less than 2 cm [48]. If more than one identified vertex passes these requirements,

the primary-event vertex is chosen as the one with the highest sum of p_{T}^2 over its constituent tracks.

Individual particle candidates are reconstructed and identified using the CMS particle-flow (PF) algorithm [49,50], by combining information from all subdetector systems. The reconstructed PF candidates are each assigned to one of the five candidate categories: electrons, muons, photons, charged hadrons, and neutral hadrons.

4.2 Lepton reconstruction and selection

Electron candidates are reconstructed by clustering the energy deposits in the ECAL and then matching the clusters with reconstructed tracks [51]. In order to suppress the multi-jet background, electron candidates must pass quality criteria tuned for high-p_{T} objects and an isolation selection [52]. The total scalar sum of the p_{T} over all the tracks in a cone of radius $\Delta R = \sqrt{(\Delta\eta)^2 + (\Delta\phi)^2} = 0.3$ around the electron direction, excluding tracks within an inner cone of $\Delta R = 0.04$ to remove the contribution from the electron itself, must be less than 5 GeV. A calorimetric isolation parameter is calculated by summing the energies of reconstructed deposits in both the ECAL and HCAL, not associated with the electron itself, within a cone of radius $\Delta R = 0.3$ around the electron. The veto threshold for this isolation parameter depends on the electron kinematic quantities and the average amount of additional energy coming from pileup interactions, calculated for each event. The electron candidates are required to have $p_{\mathrm{T}} > 90$ GeV and $|\eta| < 1.44$ or $1.57 < |\eta| < 2.5$, thus excluding the transition region between ECAL barrel and endcaps.

Muons are reconstructed with a global fit using both the tracker and muon systems [53]. An isolation requirement is applied in order to suppress the background from multi-jet events in which muons are produced in the semileptonic decay of B hadrons. A cone of radius $\Delta R = 0.3$ is constructed around the muon direction. Muon isolation requires that the scalar p_{T} sum over all tracks originating from the interaction vertex within the cone, excluding the muon itself, is less than 10 % of the p_{T} of the muon. The muon candidates are required to have $p_{\mathrm{T}} > 50$ GeV and $|\eta| < 2.1$ in each selected event.

Events are required to contain exactly one lepton candidate (electron or muon). That is, events are rejected if they contain a second lepton candidate with $p_{\mathrm{T}} > 35$ GeV (electrons) or $p_{\mathrm{T}} > 20$ GeV (muons).

4.3 Jets and missing transverse momentum reconstruction

Hadronic jets are identified by clustering PF candidates, using the FastJet v3.0.1 software package [54]. In the jet-clustering procedure, charged PF candidates associated with pileup vertices are excluded, to reduce contamination from pileup. In order to identify a Higgs boson decaying into bottom quarks, jets are clustered using the Cambridge–Aachen algorithm [55] with a distance parameter of 0.8 ("CA8 jets"). Only the highest p_{T} CA8 jet is used. Jets in the event are also identified using the anti-k_{T} jet-clustering algorithm [56] with a distance parameter of 0.5 ("AK5 jets"). AK5 jets are required to be separated from the CA8 jet by $\Delta R > 0.8$. An event-by-event correction based on the projected area of the jet on the front face of the calorimeter is used to remove the extra energy deposited in jets by neutral particles coming from pileup. Furthermore, jet energy corrections are applied, based on measurements in dijet and photon+jet events in data [57]. Additional quality criteria are applied to the jets in order to remove spurious jet-like features originating from calorimeter noise [58]. The CA8 (AK5) jets are required to be separated from the selected electron or muon candidate by $\Delta R > 0.8$ (0.3). Only jets with $p_{\mathrm{T}} > 30$ GeV and $|\eta| < 2.4$ are allowed in the subsequent steps of the analysis. Furthermore, CA8 jets are not used in the analysis if their pseudo-rapidity falls in the region $1.0 < |\eta| < 1.8$, thus overlapping the barrel-endcap transition region of the silicon tracker. In that region, 'noise' can arise when the tracking algorithm reconstructs many fake displaced tracks associated with the jet. The simulation does not sufficiently describe the full material budget of the tracking detector in that region, thus it does not accurately describe this effect. Without this requirement, a bias can be introduced in the b tagging, jet substructure and missing transverse momentum information, making this analysis systematically prone to that noise. The probability of signal events satisfying the requirement that the pseudorapidity of the CA8 jet falls outside the region $1.0 < |\eta| < 1.8$ is 80 % (92 %) for a resonance mass of 1.0 (2.5) TeV.

A b tagging algorithm, known as the combined secondary vertex algorithm [27,59], is applied to reconstructed AK5 jets to identify whether they originate from bottom quarks. This method allows the identification and rejection of the $\mathrm{t\bar{t}}$ events as described in Sect. 4.6. The chosen algorithm working point provides a misidentification rate for light-parton jets of ∼1 % and an efficiency of ∼70 % [27]. The simulated events are reweighted event-by-event with the ratio of the b tagging efficiency in data and simulation, determined in a sample enriched with b-jets. The average value of the correction factor is 0.95. The same b tagging algorithm is also used to identify whether the CA8 jet comes from a Higgs boson decaying into bottom quarks, as described in Sect. 4.5.

The missing transverse momentum $p_{\mathrm{T}}^{\mathrm{miss}}$ is defined as the magnitude of the projection on the plane perpendicular to the beams of the negative vector sum of the momenta of all the reconstructed particles in an event. The raw $p_{\mathrm{T}}^{\mathrm{miss}}$ value is modified to account for corrections to the energy-momentum scale of all the reconstructed AK5 jets in the event. More details on the $p_{\mathrm{T}}^{\mathrm{miss}}$ performance in CMS can be found in Refs. [60,61]. A requirement of $p_{\mathrm{T}}^{\mathrm{miss}} > 80\,(40)$ GeV is

applied for the electron (muon) channel. The higher threshold for the electron channel is motivated by the higher contribution from the multijet background expected in the low-$p_{\mathrm{T}}^{\mathrm{miss}}$ range due to jets misidentified as electrons. The background is expected to be negligible in the muon channel, for which a lower $p_{\mathrm{T}}^{\mathrm{miss}}$ threshold can be used to preserve a higher efficiency for a low-mass signal.

4.4 The $\mathrm{W} \to \ell\nu$ reconstruction and identification

The identified electron or muon is associated with the $\mathrm{W} \to \ell\nu$ candidate. The p_{T} of the undetected neutrino is assumed to be equal to the $p_{\mathrm{T}}^{\mathrm{miss}}$. The longitudinal component $p_{z,\nu}$ of the neutrino momentum is calculated following a method used originally for the reconstruction of the invariant mass of the top quark as described in Ref. [62]. The method aims to solve a quadratic equation that makes use of the known W boson mass. Kinematic ambiguities in the solution of the equation are resolved as in Ref. [62]. The four-momentum of the neutrino is used to build the four-momentum of the $\mathrm{W} \to \ell\nu$ candidate.

4.5 The $\mathrm{H} \to \mathrm{b\bar{b}}$ identification using jet substructure and b tagging

The CA8 jets are used to reconstruct the jet candidates from decays of Lorentz-boosted Higgs boson to bottom quarks. We exploit two techniques to discriminate against quark and gluon jets from the multijet background, including the requirement that the reconstructed jet mass be close to the Higgs boson mass, and b tagging methods that discriminate jets originating from the b quarks from those originating from lighter quarks or gluons.

First, we apply a jet-grooming technique [26,63] to recluster the jet constituents, while applying additional requirements to remove possible contamination from soft QCD radiation or pileup. Different jet-grooming algorithms have been explored at CMS, and their performance on jets in multijet processes has been studied in detail [63]. In this analysis, we use the *jet pruning* algorithm [64,65], which re-clusters each jet starting from all its original constituents using the CA algorithm iteratively, while discarding soft and large-angle recombinations at each step. The performance of the algorithm depends on the two parameters, $z_{\mathrm{cut}} = 0.1$ and $D_{\mathrm{cut}} = m_{\mathrm{jet}}/p_{\mathrm{T}}^{\mathrm{jet}}$, which define the maximum allowed hardness and the angle of the recombinations in the clustering algorithm, respectively. A jet is considered as an H-tagged jet candidate if its pruned mass, m_{jet}, computed from the sum of the four-momenta of the constituents surviving the pruning, falls in the range $110 < m_{\mathrm{jet}} < 135$ GeV. The m_{jet} window is the result of an optimization based on signal sensitivity and on the constraints due to the higher bounds of the signal regions of other diboson analyses [25].

The simulation modelling of the pruned mass measurement for merged jets from heavy bosons has been checked using merged $\mathrm{W} \to \mathrm{\bar{q}q'}$ decays in $\mathrm{t\bar{t}}$ events with a ℓ+jets topology [26]. The data are compared with $\mathrm{t\bar{t}}$ events generated with MadGraph, interfaced to Pythia for parton showering. The differences between recorded and simulated event samples in the pruned jet mass scale and resolution are found to be up to 1.7 and 11 %, respectively. In addition, the modelling of bottom quark fragmentation is checked through reconstruction of the top quark mass in these $\mathrm{t\bar{t}}$ events [66].

To discriminate between quark and gluon jets, on one hand, and a Higgs-initiated jet, on the other, formed by the hadronization of two bottom quarks, we use a H tagging technique [27]. This procedure splits the candidate H-jet into two sub-jets by reversing the last step of the CA8 pruning recombination algorithm. Depending on the angular separation ΔR of the two sub-jets, different b tagging discriminators are used to tag the H-jet candidate. If $\Delta R > 0.3$, then the b tagging algorithm is applied to both of the individual sub-jets of the CA8 jet; otherwise, it is applied to the whole CA8 jet. The chosen algorithm working point provides a misidentification rate of 10 % and an efficiency of 80 %. The ratio of the b tagging efficiency between data and simulation, in a sample enriched with b-jets from gluon splitting by requiring two muons within the CA8 jet, is used to reweight the simulated events.

4.6 Final event selection and categorization

After reconstructing the W and Higgs bosons, we apply the final selections used for the search. Both the W and Higgs boson candidates must have a p_{T} greater than 200 GeV. In addition, we apply topological selection criteria, requiring that the W and Higgs bosons are approximately back-to-back, since they tend to be isotropically distributed for background events. In particular, the ΔR distance between the lepton and the H-tagged jet must be greater than $\pi/2$, the azimuthal angular separation between the $p_{\mathrm{T}}^{\mathrm{miss}}$ and the H-tagged jet must be greater than 2.0 radians, and the azimuthal angular separation between the $\mathrm{W} \to \ell\nu$ and H-tagged jet candidates must be greater than 2.0 radians. To further reduce the level of the $\mathrm{t\bar{t}}$ background, events with one or more reconstructed AK5 jets, not overlapping with the CA8 H-tagged jet candidate as described previously in Sect. 4.3, are analyzed. If one or more of the AK5 jets is b-tagged, the event is rejected. Furthermore, a leptonically decaying top quark candidate mass m_{top}^{ℓ} is reconstructed from the lepton, $p_{\mathrm{T}}^{\mathrm{miss}}$, and the closest AK5 jet to the lepton using the method described in Ref. [62]. A hadronically decaying top quark candidate mass $m_{\mathrm{top}}^{\mathrm{h}}$ is reconstructed from the CA8 H-tagged jet candidate and the closest AK5 jet. Events with $120 < m_{\mathrm{top}}^{\ell} < 240$ GeV or $160 < m_{\mathrm{top}}^{\mathrm{h}} < 280$ GeV are rejected. The chosen windows

around the top quark mass are the result of an optimization carried out in this analysis, taking into account the asymmetric tails at larger values due to combinatorial background. If several distinct WH resonance candidates are present in the same event, only the candidate with the highest-p_T H-tagged jet is kept for further analysis. The invariant mass of the WH resonance (M_{WH}) is required to be at least 0.7 TeV. The signal efficiency for the full event selection ranges between ∼3 and ∼9 %, depending on the resonance mass.

5 Modelling of background and signal

5.1 Background estimation

After the full event selection, the two dominant remaining backgrounds are expected to come from W+jets and $t\bar{t}$ events. Backgrounds from $t\bar{t}$, single top quark, and diboson production are estimated using simulated samples after applying correction factors derived from control samples in data. For the W+jets background estimation, a procedure based on data has been developed to determine both the normalization and the M_{WH} shape.

For the W+jets normalization estimate, a signal-depleted control region is defined outside the m_{jet} mass window described in Sect. 4.5. A lower sideband region is defined in the m_{jet} range [40, 110] GeV as well as an upper sideband in the range [135, 150] GeV. The overall normalization of the W+jets background in the signal region is determined from the likelihood of the sum of backgrounds fit to the m_{jet} distribution in both sidebands of the observed data. In this approach, simulated events are replaced by an analytical function, which has been determined individually for each background process. Figure 2 shows the result of this fit procedure, where all selections are applied except the final m_{jet} signal window requirement. The inclusive W+jets background is predicted from a fit excluding the signal region (between the vertical dashed lines), while the other backgrounds are estimated from simulation.

The shape of the W+jets background as a function of M_{WH} in the signal region is estimated using the lower sideband region of the m_{jet} distribution. Correlations needed to extrapolate from the sideband to the signal region are determined from simulation through an extrapolation function defined as:

$$\alpha_{MC}(M_{WH}) = \frac{F^{W+jets}_{MC,SR}(M_{WH})}{F^{W+jets}_{MC,SB}(M_{WH})}, \quad (1)$$

where $F^{W+jets}_{MC,SR}$ and $F^{W+jets}_{MC,SB}$ are the probability density functions determined from the M_{WH} spectrum in simulation for the signal region and low-m_{jet} sideband region, respectively.

In order to estimate the W+jets contribution $F^{W+jets}_{DATA,SB}$ in the control region of the data the other backgrounds are subtracted from the observed M_{WH} distribution in the lower sideband region. The shape of the W+jets background distribution in the signal region is obtained by scaling $F^{W+jets}_{DATA,SB}$ according to α_{MC}. The final prediction of the background contribution in the signal region, N^{BKGD}_{SR}, is given by

$$N^{BKGD}_{SR}(M_{WH}) = C^{W+jets}_{SR} F^{W+jets}_{DATA,SB}(M_{WH})\,\alpha_{MC}(M_{WH}) + \sum_k C^k_{SR} F^k_{MC,SR}(M_{WH}), \quad (2)$$

where the index k runs over the list of minor backgrounds, and C^{W+jets}_{SR} and C^k_{SR} represent the normalizations of the yields of the dominant W+jets background and of the different minor background contributions. The C^{W+jets}_{SR} parameter is deter-

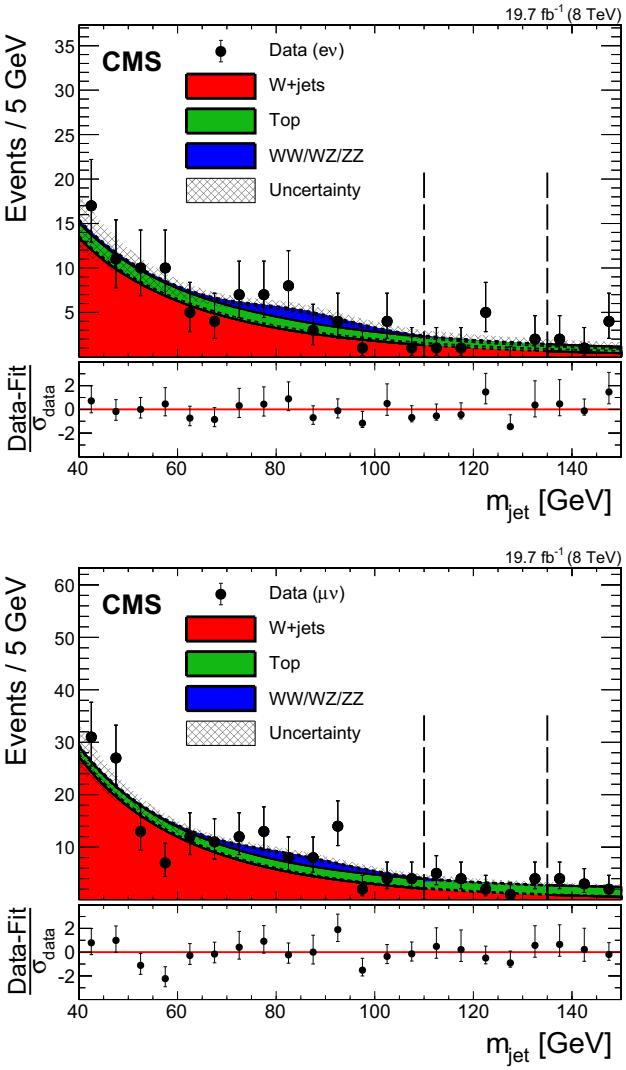

Fig. 2 Distributions of the pruned jet mass, m_{jet}, in the electron (*top*) and muon (*bottom*) channels. The signal region lies between the *dashed vertical lines*. *The hatched region* indicates the statistical uncertainty of the fit. At the bottom of each plot, the bin-by-bin fit residuals, (Data − Fit)/σ_{data}, are shown

mined from the fit to the m_{jet} distribution as described above, while each C^k_{SR} is determined from simulation. The ratio α_{MC} accounts for the small kinematic differences between signal and sideband regions, and is largely independent of the assumptions on the overall cross section. The validity and robustness of this method have been studied in data using a lower m_{jet} sideband of [40, 80] GeV to predict an alternate signal region with m_{jet} in the range [80, 110] GeV. Both the normalization and shape of the W+jets background are successfully estimated for the alternate signal region. This alternate signal region differs from the signal region of the search for WW or WZ resonances in Ref. [25] as b tagging is applied to the CA8 jet. We are therefore able to evaluate the potential WW and WZ signal contamination in the alternate signal region and find less than 5 % signal contamination, assuming a signal cross section corresponding to the exclusion limit for a WW resonance from Ref. [25]. The M_{WH} distribution of the background in the signal and lower sideband regions is described analytically by a function defined as $f(x) \propto \exp[-x/(c_0 + c_1 x)]$, which is found to describe the simulation well. Alternative fit functions have been studied but in all cases the background shapes agree with that of the default function within uncertainties.

For the $\mathrm{t\bar{t}}$ background estimate, a control sample is selected by applying all analysis requirements, except that the b-tagged jet veto is inverted, the veto on the top quark mass is dropped, and the m_{jet} requirement is removed. The data are compared with the predictions from simulation and good agreement is found. The pruned jet mass distribution in the top quark enriched control sample is shown in Fig. 3. The pruned jet mass distribution shows a small peak due to isolated W boson decays into hadrons, along with a smoothly varying combinatorial component mainly due to events in which the extra b-tagged jet from the top quark decay is in the proximity of the W boson. The difference in normalization between data and simulation is found to be 4.6 ± 5.6 %, where the quoted uncertainty is only statistical. This normalization difference is applied to correct the normalization of $\mathrm{t\bar{t}}$ background in the signal region. The relative uncertainty of 5.6 % is used to quantify the uncertainty in the $\mathrm{t\bar{t}}$ and single top quark background normalization, as described in Sect. 6.1.

5.2 Modelling of the signal mass distribution

The shape of the reconstructed signal mass distribution is extracted from the simulated signal samples. In the final analysis of the M_{WH} spectrum, the statistical signal sensitivity depends on an accurate description of the signal shape. The signal shape is parametrized with a double-sided Crystal Ball function (i.e. a Gaussian core with power-law tails on both sides) [67] to describe the CMS detector resolution. Figure 4 shows an example of this parametrization for a W′ mass of 1.5 TeV. To take into account differences between the electron and muon p_{T} resolutions at high p_{T}, the signal mass distribution is parametrized separately for events with electrons and muons. The resolution of the reconstructed M_{WH} is given by the width of the Gaussian core and is found to be 4–6 %.

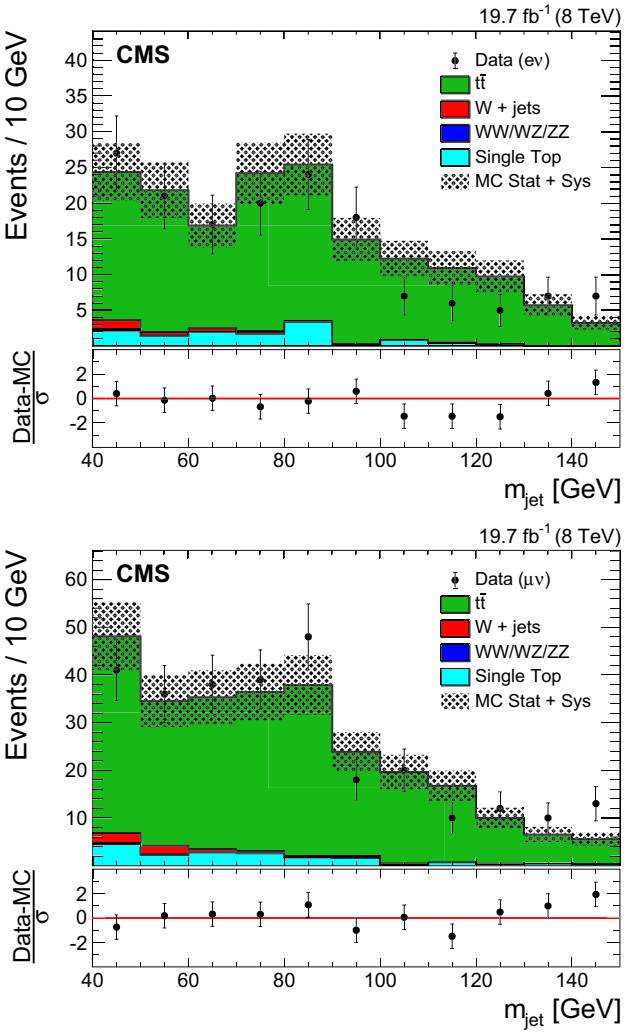

Fig. 3 Distributions of m_{jet} in the top quark enriched control sample in the electron (*top*) and muon (*bottom*) channels. *The hatched region* indicates the overall uncertainty in the background. In the lower panels, the bin-by-bin residuals, $(\text{Data} - \text{MC})/\sigma$ are shown, where σ is the sum in quadrature of the statistical uncertainty of the data, the simulation, and the systematic uncertainty in the $\mathrm{t\bar{t}}$ background

6 Systematic uncertainties

6.1 Systematic uncertainties in the background estimation

Uncertainties in the estimation of the background affect both the normalization and the shape of the M_{WH} distribution. The systematic uncertainty in the W+jets background yield is dominated by the statistical uncertainty associated with the

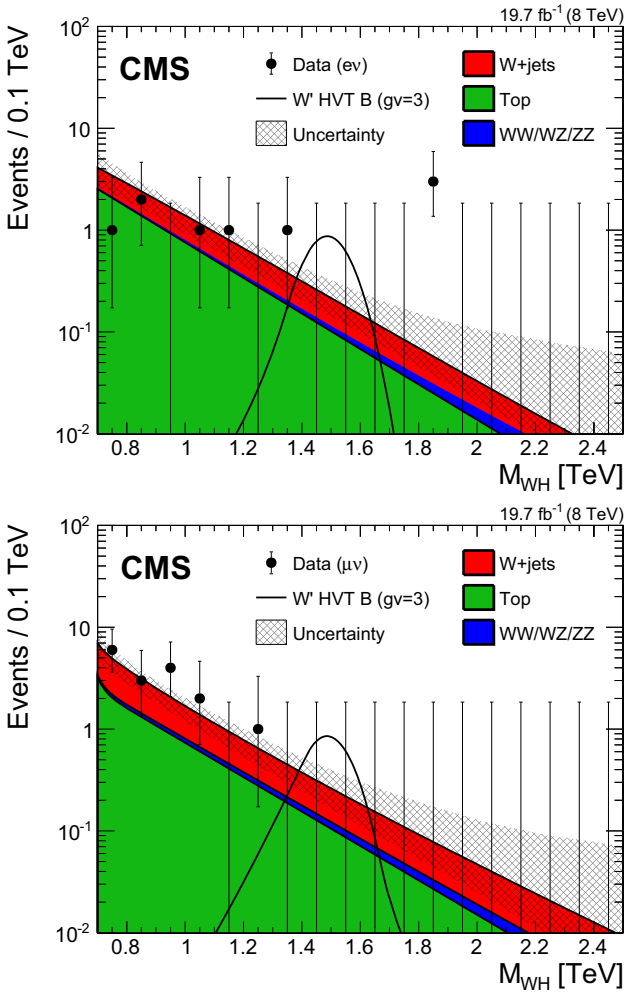

Fig. 4 Final distributions in M_{WH} for data and expected backgrounds for electron (*top*) and muon (*bottom*) categories. The 68 % error bars for Poisson event counts are obtained from the Neyman construction [77]. *The hatched region* indicates the statistical uncertainty of the fit combined with the systematical uncertainty in the shape. This figure also shows a hypothetical W′ signal with mass of 1.5 TeV, normalized to the cross section predicted by the HVT model B with parameter $g_V = 3$ as described in Sect. 8.2

number of events in data in the m_{jet} sideband regions, and it is found to be about 59 % (42 %) in the electron (muon) channel. The systematic uncertainty in the $t\bar{t}$ normalization comes from the data-to-simulation ratio derived in the top-quark-enriched control sample (5.6 %) as described in Sect. 5.1. The systematic uncertainties in the WW, WZ, and ZZ inclusive cross sections are assigned to be 10 %, taken from the relative difference in the mean value between the CMS WW cross section measurement at $\sqrt{s} = 8$ TeV and the SM expectation [68].

Systematic uncertainties in the W+jets background shape are estimated from the covariance matrix of the fit to the extrapolated data sideband and from the uncertainties in the modelling of $\alpha_{MC}(M_{WH})$. They are driven by the available data in the sidebands and the number of events generated for the simulation of the W+jets background, respectively. These uncertainties are shown in Fig. 4, and they are found to be about 30 % (120 %) at $M_{WH} \approx 1$ TeV (1.8 TeV). The estimation of the systematic uncertainty in the shape of the $t\bar{t}$ background takes into account the following contributions: the statistical uncertainty associated with the simulated event sample, the choices of regularization/factorization scales (varied up and down by a factor of 2), the matching scales in the MADGRAPH simulation, and an observed difference between MADGRAPH and POWHEG simulations.

Systematic effects from rare noise events identified in the tracker overlap region were specifically studied in the context of the acceptance requirement introduced for H-jet candidates ($|\eta| < 1.0$ or $|\eta| > 1.8$) as described in Sect. 4. Those studies conclude that any residual noise effects following the imposition of this requirement are negligible. No additional source of systematic uncertainty is taken into account for the background predictions.

6.2 Systematic uncertainties in the signal prediction

Systematic uncertainties in the signal prediction affect both the signal efficiency and the M_{WH} shape. The primary uncertainties in signal yields are summarized in Table 1 and described below.

The systematic uncertainties in the signal efficiency due to the electron energy (E) and muon p_T scales are evaluated by varying the lepton E or p_T within one standard deviation of the corresponding uncertainty [51,53]; the uncertainties due to the electron E and muon p_T resolutions are estimated applying a p_T and E smearing, respectively. In this process, variations in the lepton E or p_T are propagated consistently to the p_T^{miss} vector. We also take into account the systematic

Table 1 Summary of the systematic uncertainties in the signal yield, relative to the expected number of events

Source	Uncertainty [%]	
	Electron	Muon
Lepton trigger and ID efficiencies	3	2
Lepton p_T scale	<0.5	1
Lepton p_T resolution	<0.1	<0.1
Jet energy-momentum scale	1–3	
Jet energy-momentum resolution	<0.5	
Higgs boson mass tagging efficiency	2–10	
Higgs boson b tagging efficiency	2–8	
Unclustered energy scale	<0.5	
Pileup	0.5	
PDF	<0.5	
Integrated luminosity	2.6	

uncertainties affecting the observed-to-simulated scale factors for the efficiencies of the lepton trigger, identification and isolation requirements. These efficiencies are derived using a specialized tag-and-probe analysis with $Z \to \ell^+\ell^-$ events [69], and the uncertainty in the ratio of the efficiencies is taken as the systematic uncertainty. The uncertainties in the efficiencies of the electron (muon) trigger and the electron (muon) identification with isolation are 3 % (3 %) and 3 % (4 %), respectively.

The signal efficiency is also affected by the uncertainties in the jet energy-momentum scale and resolution. The jet energy-momentum scale and resolution are varied within their p_T- and η-dependent uncertainties [57] to estimate their impact on the signal efficiency. The variations are also propagated consistently to the p_T^{miss} vector.

The momentum scale uncertainty of particles that are not identified as leptons or clustered in jets ('unclustered energy-momentum') is found to introduce an uncertainty of less than 0.5 % in the signal efficiency.

We also include systematic uncertainties in the signal efficiency due to uncertainties in data-to-simulation scale factors for the pruned jet mass tagging, derived from the top quark enriched control sample [26] and b-tagged jet identification efficiencies [27]. These sources introduce a systematic uncertainty in the mass tagging and b tagging of the Higgs boson of 2–10 % and 2–8 %, respectively, depending on the signal mass.

The systematic uncertainty due to the modelling of pileup is estimated by reweighting the signal simulation samples such that the distribution of the number of interactions per bunch crossing is shifted according to the uncertainty in the inelastic proton–proton cross section [70,71].

The impact of the proton PDF uncertainties on the signal efficiency is evaluated with the PDF4LHC prescription [72,73], using the MSTW2008 [74] and NNPDF2.1 [75] PDF sets. The uncertainty in the integrated luminosity is 2.6 % [76].

In addition to systematic uncertainties in the signal efficiency discussed above, we consider uncertainties in the signal resonance peak position and width. The systematic effects that could change the signal shape are the uncertainties due to the p_T/energy-momentum scale and resolution of electrons, muons, jets, and the unclustered energy-momentum scale. For each of these sources of experimental uncertainty, the energy-momentum of the lepton and jets, as well as the corresponding p_T^{miss} vector, are varied (or smeared) by their relative uncertainties. The uncertainty in the peak position of the signal is estimated to be less than 1 %. The jet energy-momentum scale and resolution introduce a relative uncertainty of about 3 % in the signal width. The unclustered energy-momentum scale introduces an uncertainty in the signal width of 1 % at lower resonance masses (<1.5 TeV), and of 3 % at higher masses.

Table 2 Observed and expected yields in the signal region together with statistical uncertainties

	eν+H-jet	$\mu\nu$+H-jet
Observed yield	9	16
Expected total background	11.3 ± 3.1	14.9 ± 3.1
W+jets	4.7 ± 2.9	7.0 ± 3.1
Top	6.3 ± 1.1	7.3 ± 0.4
VV	0.4 ± 0.1	0.6 ± 0.2

7 Results

The predicted number of background events in the signal region after the inclusion of all backgrounds is summarized in Table 2 and compared with observations. The yields are quoted in the range $0.7 < M_{WH} < 3$ TeV. The expected background is derived with the sideband procedure. The uncertainties in the background prediction from data are statistical in nature, as they depend on the number of events in the sideband region. The muon channel has more expected background events than the electron channel owing to the lower p_T^{miss} requirement on the muon and its worse mass resolution at high p_T.

Figure 4 shows the M_{WH} spectra after all selection criteria have been applied. The highest mass event is in the electron category and has $M_{WH} \approx 1.9$ TeV. The observed data and the predicted background in the muon channel agree. In the electron channel, an excess of three events is observed with $M_{WH} > 1.8$ TeV, where about 0.3 events are expected, while in the muon channel no events with $M_{WH} > 1.8$ TeV are observed, where about 0.3 events are expected.

8 Statistical and model interpretation

8.1 Significance of the data

A comparison between the M_{WH} distribution observed in data and the largely data-driven background prediction is used to test for the presence of a resonance decaying into WH. The statistical test is performed based on a profile likelihood discriminant that describes an unbinned shape analysis. Systematic uncertainties in the signal and background yields are treated as nuisance parameters and profiled in the statistical interpretation using log-normal priors.

We evaluate the local significance of the observations in the context of the described test, under the assumptions of a narrow resonance decaying into the WH final state and lepton universality for the W boson decay, by combining the two event categories. Correlations arising from the uncertainties common to both channels are taken into account. The result is shown in Fig. 5. The highest local significance of 2.2 standard

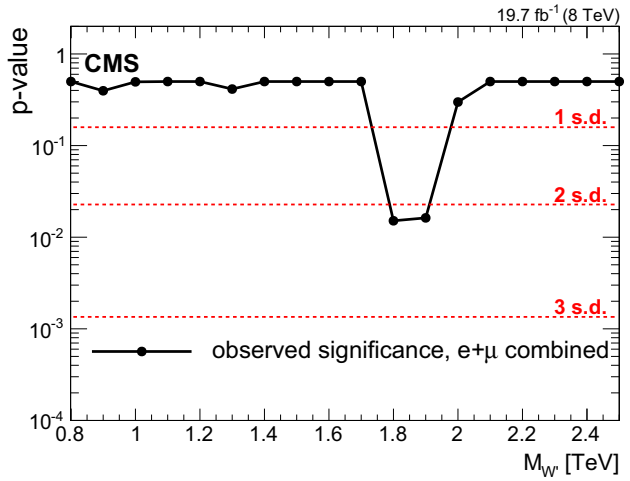

Fig. 5 Local p-value of the combined electron and muon data as a function of the W′ boson mass, probing a narrow WH resonance

deviations is found for a resonance mass of 1.8 TeV, driven by the excess in the electron channel described in Sect. 7. The corresponding local significance for a resonance of 1.8 TeV in the electron channel is 2.9 standard deviations, while in the muon channel there is no significance. Taking into account the look-elsewhere effect [78], a local significance of 2.9 standard deviations translates into a global significance of about 1.9 standard deviations searching for resonances over the full mass range 0.8–2.5 TeV and across two channels. We conclude that the results are thus statistically compatible with the SM expectation within 2 standard deviations.

8.2 Cross section limits

We set upper limits on the production cross section of a new resonance following the modified-frequentist CL_s method [79,80]. Exclusion limits can be set as a function of the W′ boson mass, under the narrow-width approximation. The results are interpreted in the HVT model B [15] which mimics the properties of composite Higgs scenarios, and in the context of the little Higgs model [8]. Typical parameter values for the HVT model B are

$$|c_H| \approx |c_F| \approx 1, \quad g_V \geq 3, \tag{3}$$

where c_H describes interactions involving the Higgs boson or longitudinally polarized SM vector bosons, c_F describes the direct interactions of the W′ with fermions, and g_V is the typical strength of the new interaction. In this scenario, decays of the W′ boson into a diboson are dominant and the W′ → WH branching fraction is almost equal to that of the decay into WZ. The parameter points for this scenario are currently not well constrained from experiments [15] because of the suppressed fermionic couplings of the W′ boson.

The following parameters are used for interpretation of the results: $g_V = 3$, $c_H = -1$ and $c_F = 1$ in the HVT model B and $\cot 2\theta = 2.3$, $\cot\theta = -0.20799$ in the LH model, where

Table 3 Intrinsic total widths (Γ) and cross sections (σ) for the LH model and HVT model B for different resonance masses. The WH → $\ell\nu b\bar{b}$ branching fraction is not included in the calculation

Resonance mass [TeV]	LH model		HVT model B	
	Γ [GeV]	σ [pb]	Γ [GeV]	σ [pb]
0.8	7.22	5.09×10^{-1}	24.1	3.37×10^{-1}
0.9	8.12	3.03×10^{-1}	27.1	2.48×10^{-1}
1.0	9.02	1.87×10^{-1}	30.1	1.71×10^{-1}
1.1	9.92	1.18×10^{-1}	33.1	1.16×10^{-1}
1.2	10.8	7.65×10^{-2}	36.1	8.05×10^{-2}
1.3	11.7	5.06×10^{-2}	39.1	5.59×10^{-2}
1.4	12.6	3.39×10^{-2}	42.2	3.88×10^{-2}
1.5	13.5	2.29×10^{-2}	45.2	2.51×10^{-2}
1.6	14.4	1.56×10^{-2}	48.2	1.87×10^{-2}
1.7	15.3	1.08×10^{-2}	51.2	1.30×10^{-2}
1.8	16.2	7.43×10^{-3}	54.2	9.03×10^{-3}
1.9	17.1	5.17×10^{-3}	57.2	6.27×10^{-3}
2.0	18.0	3.61×10^{-3}	60.2	4.25×10^{-3}
2.1	19.0	2.53×10^{-3}	63.2	3.02×10^{-3}
2.2	19.8	1.76×10^{-3}	66.2	2.10×10^{-3}
2.3	20.8	1.24×10^{-3}	69.2	1.46×10^{-3}
2.4	21.6	8.67×10^{-4}	72.2	1.01×10^{-3}
2.5	22.6	6.07×10^{-4}	75.3	7.31×10^{-4}

θ is a mixing angle parameter that determines W′ couplings and that cot 2θ and cot θ can be directly related to c_H and c_F.

The intrinsic width and cross section for both models are listed in Table 3 for several resonance masses. The widths for the HVT model B are computed by means of Eqs. (2.25) and (2.31) in Ref. [15], while the cross sections were obtained using the online tools provided by the authors of Ref. [15]. The width is less than 5 % for the following parameter values: $0.95 < g_V < 3.76$, $c_H = -1$, and $c_F = 1$; $g_V < 3.9$, $c_H = -1$, and $c_F = 0$; or $g_V < 7.8$, $c_H = 0.5$, and $c_F = 0$. The widths for the LH model have been computed by means of Eq. (15) in Ref. [81], and they are less than 5 % for values of $0.084 < |\cot\theta| < 1.21$. Hence, in both models we can consider the width to be negligible compared to the experimental resolution.

Figure 6 shows the expected and observed exclusion limits at 95 % confidence level (CL) on the product of the W′ production cross section and the branching fraction of W′ → WH for the electron and muon channels separately, and for the combination of the two. For the combined channels, the observed and expected lower limits on the W′ mass are 1.4 TeV in the LH model and 1.5 TeV in the HVT model B. For the electron (muon) channel, the observed and expected lower limits on the W′ mass are 1.2 (1.3) TeV in the LH model and 1.3 (1.3) TeV in the HVT model B.

8.3 Analysis combination

The limits obtained in this analysis can be combined with two previous results [22,24], setting limits on the sum of W′ → WH and Z′ → ZH production in the context of the HVT model. The search for $W'/Z' \to WH/ZH \to q'\bar{q}b\bar{b}/q\bar{q}q\bar{q}q\bar{q}$ [22] reports limits in the context of the HVT model that can be directly used in the combination. However, while an asymptotic approximation of the CL_s procedure was used in the original paper, for the combination the limit is re-evaluated with the CL_s procedure reported above. The search for $Z' \to ZH \to q\bar{q}\tau^+\tau^-$ [24], does not report limits in the context of a W′ resonance. However, since it is also sensitive to a signal from $W' \to WH \to q'\bar{q}\tau^+\tau^-$ with an efficiency of about 5 % less than for the Z′ signal, it was reinterpreted for the purpose of the combination. The results of the combination are shown in Fig. 7. The limit on the mass of the W′/Z′ is slightly improved to 1.8 TeV compared to the most stringent result reported by the $W'/Z' \to WH/ZH \to q'\bar{q}b\bar{b}/q\bar{q}q\bar{q}q\bar{q}$ search.

In Fig. 8, a scan of the coupling parameters and the corresponding observed 95 % CL exclusion contours in the HVT model from the combination of the analyses are shown. The parameters are defined as $g_V c_H$ and $g^2 c_F/g_V$, related to the coupling strengths of the new resonance to the Higgs boson and to fermions. The range of the scan is limited by the assumption that the new resonance is narrow. A contour is overlaid, representing the region where the theoretical width is larger than the experimental resolution of the searches, and hence where the narrow-resonance assumption is not satis-

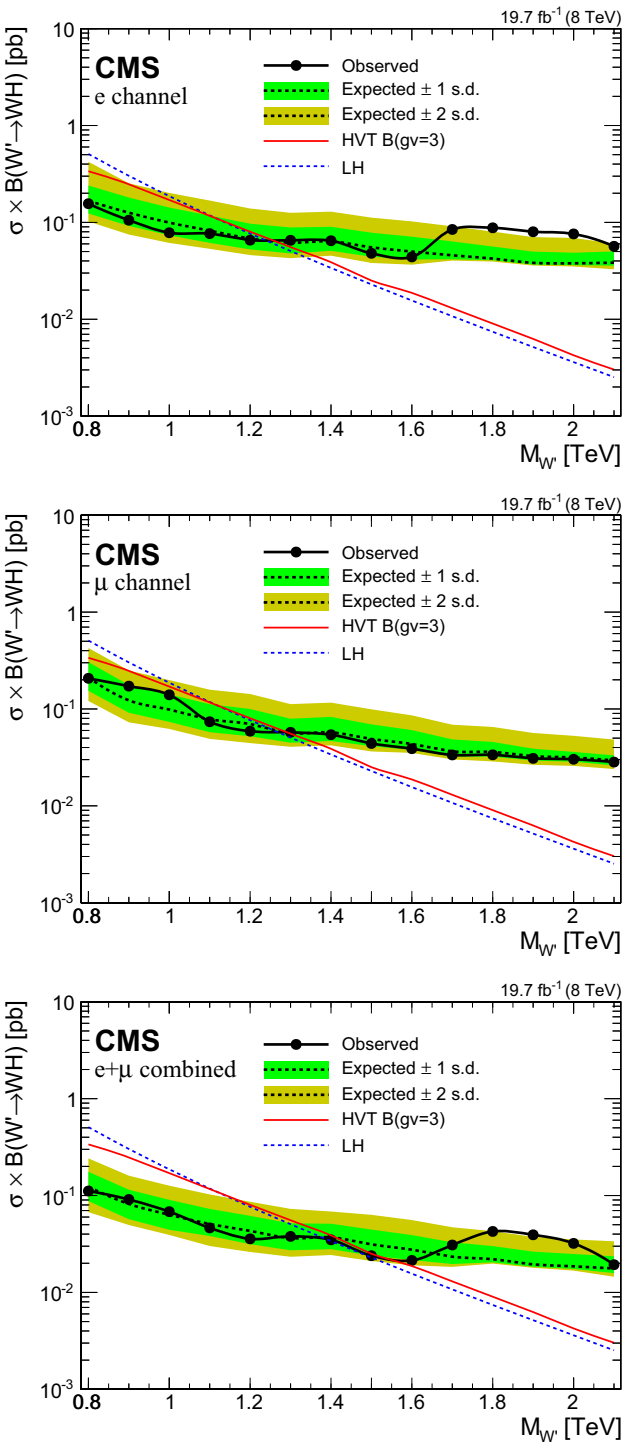

Fig. 6 Observed (*solid*) and expected (*dashed*) upper limits at 95 % CL on the product of the W′ production cross section and the branching fraction of W′ → WH for electron (*top*) and muon (*middle*) channels, and the combination of the two channels (*lower plot*). The products of cross sections and branching fractions for W′ production in the LH and HVT models are overlaid

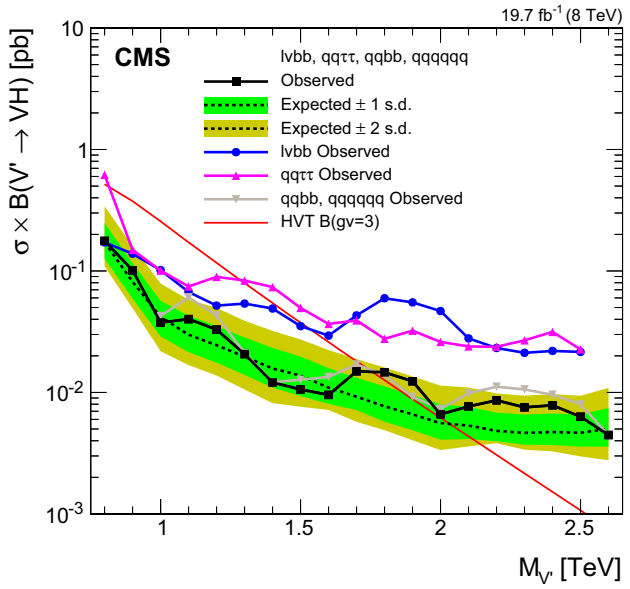

Fig. 7 Observed (*full rectangles*) and expected (*dashed line*) combined upper limits at 95 % CL on the sum of the W′ and Z′ production cross sections, weighted by their respective branching fraction of W′ → WH and Z′ → ZH. The cross section for the production of a W′ and Z′ in the HVT model B, multiplied by its branching fraction for the relevant process, is overlaid. The observed limits of the three analyses entering the combination in the final states, $\ell\nu b\bar{b}$ (*full circle*), $q\bar{q}\tau^+\tau^-$ [24] (*full triangle pointing up*), and $q\bar{q}b\bar{b}/q\bar{q}q\bar{q}q\bar{q}$ [22] (*full triangle pointing down*), are overlaid

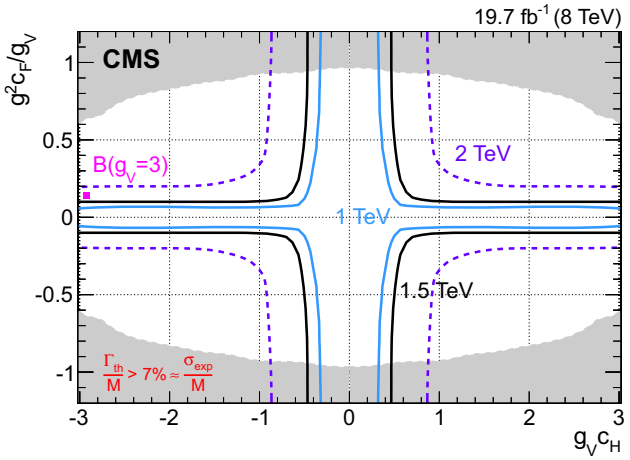

Fig. 8 Exclusion regions in the plane of the HVT-model couplings ($g_V c_H$, $g^2 c_F/g_V$) for three resonance masses, 1, 1.5, and 2 TeV, where g denotes the weak gauge coupling. The point B of the benchmark model used in the analysis is also shown. The boundaries of the regions outside these lines are excluded by this search are indicated by the *solid* and *dashed lines* (region outside these lines is excluded). The areas indicated by the *solid shading* correspond to regions where the resonance width is predicted to be more than 7 % of the resonance mass and the narrow-resonance assumption is not satisfied

fied. This contour is defined by a predicted resonance width of 7 %, corresponding to the largest resonance mass resolution of the considered searches.

9 Summary

A search has been presented for new resonances decaying into WH, in which the W boson decays into $\ell\nu$ with $\ell = e, \mu$ and the Higgs boson decays to a pair of bottom quarks. Each event is reconstructed as a leptonic W boson candidate recoiling against a jet with mass compatible with the Higgs boson mass. A specialized b tagging method for Lorentz-boosted Higgs bosons is used to further reduce the background from multijet processes. No excess of events above the standard model prediction is observed in the muon channel, while an excess with a local significance of 2.9 standard deviations is observed in the electron channel near $M_{WH} \approx 1.8$ TeV. The results are statistically compatible with the standard model within 2 standard deviations. In the context of the little Higgs and the heavy vector triplet models, upper limits at 95 % confidence level are set on the W′ production cross section in a range from 100 to 10 fb for masses between 0.8 and 2.5 TeV, respectively. Within the little Higgs model, a lower limit on the W′ mass of 1.4 TeV has been set. A heavy vector triplet model that mimics the properties of composite Higgs models has been excluded up to a W′ mass of 1.5 TeV. In this latter context, the results have been combined with related searches, improving the lower limit up to ≈1.8 TeV. This combined limit is the most restrictive to date for W′ decays to a pair of standard model bosons.

Acknowledgments We congratulate our colleagues in the CERN accelerator departments for the excellent performance of the LHC and thank the technical and administrative staffs at CERN and at other CMS institutes for their contributions to the success of the CMS effort. In addition, we gratefully acknowledge the computing centres and personnel of the Worldwide LHC Computing Grid for delivering so effectively the computing infrastructure essential to our analyses. Finally, we acknowledge the enduring support for the construction and operation of the LHC and the CMS detector provided by the following funding agencies: BMWFW and FWF (Austria); FNRS and FWO (Belgium); CNPq, CAPES, FAPERJ, and FAPESP (Brazil); MES (Bulgaria); CERN; CAS, MoST, and NSFC (China); COLCIENCIAS (Colombia); MSES and CSF (Croatia); RPF (Cyprus); MoER, ERC IUT and ERDF (Estonia); Academy of Finland, MEC, and HIP (Finland); CEA and CNRS/IN2P3 (France); BMBF, DFG, and HGF (Germany); GSRT (Greece); OTKA and NIH (Hungary); DAE and DST (India); IPM (Iran); SFI (Ireland); INFN (Italy); MSIP and NRF (Republic of Korea); LAS (Lithuania); MOE and UM (Malaysia); CINVESTAV, CONACYT, SEP, and UASLP-FAI (Mexico); MBIE (New Zealand); PAEC (Pakistan); MSHE and NSC (Poland); FCT (Portugal); JINR (Dubna); MON, RosAtom, RAS and RFBR (Russia); MESTD (Serbia); SEIDI and CPAN (Spain); Swiss Funding Agencies (Switzerland); MST (Taipei); ThEPCenter, IPST, STAR and NSTDA (Thailand); TUBITAK and TAEK (Turkey); NASU and SFFR (Ukraine); STFC (United Kingdom); DOE and NSF (USA). Individuals have received support from the Marie-Curie programme and the European Research Council and EPLANET (European Union); the Leventis Foundation; the A. P. Sloan Foundation; the Alexander von Humboldt Foundation; the Belgian Federal Science Policy Office; the Fonds pour la Formation à la Recherche dans l'Industrie et dans l'Agriculture (FRIA-Belgium); the Agentschap voor Innovatie door Wetenschap en Technologie (IWT-Belgium); the Ministry of Education, Youth and Sports (MEYS) of the Czech Republic;

the Council of Science and Industrial Research, India; the HOMING PLUS programme of the Foundation for Polish Science, cofinanced from European Union, Regional Development Fund; the OPUS programme of the National Science Center (Poland); the Compagnia di San Paolo (Torino); MIUR project 20108T4XTM (Italy); the Thalis and Aristeia programmes cofinanced by EU-ESF and the Greek NSRF; the National Priorities Research Program by Qatar National Research Fund; the Rachadapisek Sompot Fund for Postdoctoral Fellowship, Chulalongkorn University (Thailand); the Chulalongkorn Academic into Its 2nd Century Project Advancement Project (Thailand); and the Welch Foundation, contract C-1845.

References

1. CMS Collaboration, Observation of a new boson at a mass of 125 GeV with the CMS experiment at the LHC. Phys. Lett. B **716**, 30 (2012). doi:10.1016/j.physletb.2012.08.021. arXiv:1207.7235
2. ATLAS Collaboration, Observation of a new particle in the search for the Standard Model Higgs boson with the ATLAS detector at the LHC. Phys. Lett. B **716**, 1 (2012). doi:10.1016/j.physletb.2012.08.020. arXiv:1207.7214
3. CMS Collaboration, Observation of a new boson with mass near 125 GeV in pp collisions at $\sqrt{s} = 7$ and 8 TeV. JHEP **06**, 081 (2013). doi:10.1007/JHEP06(2013)081. arXiv:1303.4571
4. ATLAS and CMS Collaborations, Combined measurement of the Higgs boson mass in pp collisions at $\sqrt{s} = 7$ and 8 TeV with the ATLAS and CMS experiments. Phys. Rev. Lett. **114**, 191803 (2015). doi:10.1103/PhysRevLett.114.191803. arXiv:1503.07589
5. B. Bellazzini, C. Csaki, J. Serra, Composite Higgses. Eur. Phys. J. C **74**, 2766 (2014). doi:10.1140/epjc/s10052-014-2766-x. arXiv:1401.2457
6. R. Contino, D. Marzocca, D. Pappadopulo, R. Rattazzi, On the effect of resonances in composite Higgs phenomenology. JHEP **10**, 081 (2011). doi:10.1007/JHEP10(2011)081. arXiv:1109.1570
7. D. Marzocca, M. Serone, J. Shu, General composite Higgs models. JHEP **08**, 013 (2012). doi:10.1007/JHEP08(2012)013. arXiv:1205.0770
8. T. Han, H.E. Logan, B. McElrath, L.-T. Wang, Phenomenology of the little Higgs model. Phys. Rev. D **67**, 095004 (2003). doi:10.1103/PhysRevD.67.095004. arXiv:hep-ph/0301040
9. M. Perelstein, Little Higgs models and their phenomenology. Prog. Part. Nucl. Phys. **58**, 247 (2005). doi:10.1016/j.ppnp.2006.04.001. arXiv:hep-ph/0512128
10. M. Schmaltz, D. Tucker-Smith, Little Higgs review. Ann. Rev. Nucl. Part. Sci. **55**, 229 (2005). doi:10.1146/annurev.nucl.55.090704.151502. arXiv:hep-ph/0502182
11. N. Arkani-Hamed, A.G. Cohen, E. Katz, A.E. Nelson, The littlest Higgs. JHEP **07**, 034 (2002). doi:10.1088/1126-6708/2002/07/034. arXiv:hep-ph/0206021
12. K. Lane, A composite Higgs model with minimal fine-tuning: the large-N and weak-technicolor limit. Phys. Rev. D **90**, 095025 (2014). doi:10.1103/PhysRevD.90.095025. arXiv:1407.2270
13. K. Lane, L. Prichett, Heavy vector partners of the light composite Higgs. Phys. Lett. B **753**, 211 (2016). doi:10.1016/j.physletb.2015.12.003. arXiv:1507.07102
14. B.A. Dobrescu, Z. Liu, Heavy Higgs bosons and the 2 TeV W′ boson. JHEP **02**, 118 (2015). doi:10.1007/JHEP10(2015)118. arXiv:1507.01923
15. D. Pappadopulo, A. Thamm, R. Torre, A. Wulzer, Heavy vector triplets: bridging theory and data. JHEP **09**, 060 (2014). doi:10.1007/JHEP09(2014)060. arXiv:1402.4431
16. CMS Collaboration, Search for physics beyond the standard model in final states with a lepton and missing transverse energy in proton-proton collisions at $\sqrt{s} = 8$ TeV. Phys. Rev. D **91**, 092005 (2015). doi:10.1103/PhysRevD.91.092005. arXiv:1408.2745
17. ATLAS Collaboration, Search for new particles in events with one lepton and missing transverse momentum in pp collisions at $\sqrt{s} =$ 8 TeV with the ATLAS detector. JHEP **09**, 037 (2014). doi:10.1007/JHEP09(2014)037. arXiv:1407.7494
18. CMS Collaboration, Search for massive resonances in dijet systems containing jets tagged as W or Z boson decays in pp collisions at $\sqrt{s}$= 8 TeV. J. High Energy Phys. **08**, 173 (2014). doi:10.1007/JHEP08(2014)173
19. CMS Collaboration, Search for new resonances decaying to WZ in proton–proton collisions at $\sqrt{s} = 8$ TeV. Phys. Lett. B **740**, 83 (2015). doi:10.1016/j.physletb.2014.11.026. arXiv:1407.3476
20. ATLAS Collaboration, Search for production of WW/WZ resonances decaying to a lepton, neutrino and jets in pp collisions at $\sqrt{s} = 8$ TeV with the ATLAS detector. Eur. Phys. J. C **75**, 209 (2015). doi:10.1140/epjc/s10052-015-3425-6. arXiv:1503.04677
21. ATLAS Collaboration, Search for WZ resonances in the fully leptonic channel using pp collisions at $\sqrt{s} = 8$ TeV with the ATLAS detector. Phys. Lett. B **737**, 223 (2014). doi:10.1016/j.physletb.2014.08.039. arXiv:1406.4456
22. CMS Collaboration, Search for a massive resonance decaying into a Higgs boson and a W or Z boson in hadronic final states in proton–proton collisions at $\sqrt{s} = 8$ TeV. JHEP **02**, 145 (2016). doi:10.1007/JHEP02(2016)145. arXiv:1506.01443
23. ATLAS Collaboration, Search for a new resonance decaying to a W or Z boson and a Higgs boson in the $\ell\ell/\ell\nu/\nu\nu + b\bar{b}$ final states with the ATLAS detector. Eur. Phys. J. C **75**, 263 (2015). doi:10.1140/epjc/s10052-015-3474-x. arXiv:1503.08089
24. CMS Collaboration, Search for narrow high-mass resonances in proton-proton collisions at $\sqrt{s} = 8$ TeV decaying to a Z and a Higgs boson. Phys. Lett. B **748**, 255 (2015). doi:10.1016/j.physletb.2015.07.011
25. CMS Collaboration, Search for massive resonances decaying into pairs of boosted bosons in semi-leptonic final states at $\sqrt{s} = 8$TeV. J. High Energy Phys. **08**, 174 (2014). doi:10.1007/JHEP08(2014)174
26. CMS Collaboration, Identification techniques for highly boosted W bosons that decay into hadrons. J. High Energy Phys. **12**, 017 (2014). doi:10.1007/JHEP12(2014)017
27. CMS Collaboration, Performance of b tagging at $\sqrt{s} = 8$ TeV in multijet, $t\bar{t}$ and boosted topology events. CMS Physics Analysis Summary CMS-PAS-BTV-13-001 (2013)
28. CMS Collaboration, The CMS experiment at the CERN LHC. JINST **3**, S08004 (2008). doi:10.1088/1748-0221/3/08/S08004
29. J. Alwall et al., MadGraph 5: going beyond. JHEP **06**, 128 (2011). doi:10.1007/JHEP06(2011)128. arXiv:1106.0522
30. P. Nason, A new method for combining NLO QCD with shower Monte Carlo algorithms. JHEP **11**, 040 (2004). doi:10.1088/1126-6708/2004/11/040. arXiv:hep-ph/0409146
31. S. Frixione, P. Nason, C. Oleari, Matching NLO QCD computations with parton shower simulations: the POWHEG method. JHEP **07**, 070 (2007). doi:10.1088/1126-6708/2007/11/070. arXiv:0709.2092
32. S. Alioli, P. Nason, C. Oleari, E. Re, A general framework for implementing NLO calculations in shower Monte Carlo programs: the POWHEG BOX. JHEP **06**, 043 (2010). doi:10.1007/JHEP06(2010)043. arXiv:1002.2581

33. S. Alioli, P. Nason, C. Oleari, E. Re, NLO single-top production matched with shower in POWHEG: s- and t-channel contributions. JHEP **09**, 111 (2009). doi:10.1088/1126-6708/2009/09/111. arXiv:0907.4076. [Erratum: doi:10.1007/JHEP02(2010)011]
34. E. Re, Single-top W t-channel production matched with parton showers using the POWHEG method. Eur. Phys. J. C **71**, 1547 (2011). doi:10.1140/epjc/s10052-011-1547-z. arXiv:1009.2450
35. S. Alioli, S.-O. Moch, P. Uwer, Hadronic top-quark pair-production with one jet and parton showering. JHEP **01**, 137 (2012). doi:10.1007/JHEP01(2012)137. arXiv:1110.5251
36. T. Sjöstrand, S. Mrenna, P. Skands, PYTHIA 6.4 physics and manual. JHEP **05**, 026 (2006). doi:10.1088/1126-6708/2006/05/026. arXiv:hep-ph/0603175
37. J. Pumplin et al., New generation of parton distributions with uncertainties from global QCD analysis. JHEP **07**, 012 (2002). doi:10.1088/1126-6708/2002/07/012. arXiv:hep-ph/0201195
38. H.-L. Lai et al., New parton distributions for collider physics. Phys. Rev. D **82**, 074024 (2010). doi:10.1103/PhysRevD.82.074024. arXiv:1007.2241
39. CMS Collaboration, Measurement of the underlying event activity at the LHC with $\sqrt{s} = 7$ TeV and comparison with $\sqrt{s} = 0.9$ TeV. JHEP **09**, 109 (2011). doi:10.1007/JHEP09(2011)109. arXiv:1107.0330
40. CMS Collaboration, Study of the underlying event at forward rapidity in pp collisions at $\sqrt{s} = 0.9$, 2.76, and 7 TeV. JHEP **04**, 072 (2013). doi:10.1007/JHEP04(2013)072. arXiv:1302.2394
41. GEANT4 Collaboration, GEANT4—a simulation toolkit. Nucl. Instrum. Methods A **506**, 250 (2003). doi:10.1016/S0168-9002(03)01368-8
42. J.M. Campbell, R.K. Ellis, D.L. Rainwater, Next-to-leading order QCD predictions for $W + 2$ jet and $Z + 2$ jet production at the CERN LHC. Phys. Rev. D **68**, 094021 (2003). doi:10.1103/PhysRevD.68.094021. arXiv:hep-ph/0308195
43. J.M. Campbell, R.K. Ellis, C. Williams, Vector boson pair production at the LHC. JHEP **07**, 018 (2011). doi:10.1007/JHEP07(2011)018. arXiv:1105.0020
44. J.M. Campbell, R.K. Ellis, Top-quark processes at NLO in production and decay. J. Phys. G **42**, 015005 (2015). doi:10.1088/0954-3899/42/1/015005. arXiv:1204.1513
45. J.M. Campbell, R.K. Ellis, T. Francesco, Single top production and decay at next-to-leading order. Phys. Rev. D **70**, 094012 (2004). doi:10.1103/PhysRevD.70.094012. arXiv:hep-ph/0408158
46. Y. Li, F. Petriello, Combining QCD and electroweak corrections to dilepton production in FEWZ. Phys. Rev. D **86**, 094034 (2012). doi:10.1103/PhysRevD.86.094034. arXiv:1208.5967
47. M. Czakon, A. Mitov, Top++: a program for the calculation of the top-pair cross-section at hadron colliders. Comput. Phys. Commun. **185**, 2930 (2014). doi:10.1016/j.cpc.2014.06.021. arXiv:1112.5675
48. CMS Collaboration, Description and performance of track and primary-vertex reconstruction with the CMS tracker. JINST **9**, P10009 (2014). doi:10.1088/1748-0221/9/10/P10009. arXiv:1405.6569
49. CMS Collaboration, Particle-flow event reconstruction in CMS and performance for jets, taus, and $E_{\mathrm{T}}^{\mathrm{miss}}$. CMS Physics Analysis Summary CMS-PAS-PFT-09-001 (2009)
50. CMS Collaboration, Commissioning of the Particle-flow Event Reconstruction with the first LHC collisions recorded in the CMS detector. CMS Physics Analysis Summary CMS-PAS-PFT-10-001 (2010)
51. CMS Collaboration, Performance of electron reconstruction and selection with the CMS detector in proton–proton collisions at $\sqrt{s} = 8$ TeV. JINST **10**, P06005 (2015). doi:10.1088/1748-0221/10/06/P06005. arXiv:1502.02701
52. CMS Collaboration, Search for leptonic decays of W′ bosons in pp collisions at $\sqrt{s} = 7$ TeV. JHEP **08**, 023 (2012). doi:10.1007/JHEP08(2012)023. arXiv:1204.4764
53. CMS Collaboration, Performance of CMS muon reconstruction in pp collision events at $\sqrt{s} = 7$ TeV. JINST **7**, P10002 (2012). doi:10.1088/1748-0221/7/10/P10002. arXiv:1206.4071
54. M. Cacciari, G.P. Salam, G. Soyez, FastJet user manual. Eur. Phys. J. C **72**, 1896 (2012). doi:10.1140/epjc/s10052-012-1896-2. arXiv:1111.6097
55. M. Wobisch, T. Wengler, Hadronization corrections to jet cross-sections in deep inelastic scattering (1998). arXiv:hep-ph/9907280
56. M. Cacciari, G.P. Salam, G. Soyez, The anti-k_t jet clustering algorithm. JHEP **04**, 063 (2008). doi:10.1088/1126-6708/2008/04/063. arXiv:0802.1189
57. CMS Collaboration, Determination of jet energy calibration and transverse momentum resolution in CMS. JINST **6**, P11002 (2011). doi:10.1088/1748-0221/6/11/P11002. arXiv:1107.4277
58. CMS Collaboration, Jet performance in pp collisions at $\sqrt{s} = 7$ TeV. CMS Physics Analysis Summary CMS-PAS-JME-10-003 (2010)
59. CMS Collaboration, Identification of b-quark jets with the CMS experiment. JINST **8**, P04013 (2013). doi:10.1088/1748-0221/8/04/P04013. arXiv:1211.4462
60. CMS Collaboration, Missing transverse energy performance of the CMS detector. JINST **6**, P09001 (2011). doi:10.1088/1748-0221/6/09/P09001. arXiv:1106.5048
61. CMS Collaboration, Performance of missing transverse momentum reconstruction algorithms in proton–proton collisions at $\sqrt{s} = 8$ TeV with the CMS detector. CMS Physics Analysis Summary CMS-PAS-JME-12-002 (2012)
62. J. Bauer, Prospects for the observation of electroweak top-quark production with the CMS experiment. PhD thesis, Karlsruher Institut für Technologie (KIT) (2010)
63. CMS Collaboration, Studies of jet mass in dijet and W/Z + jet events. JHEP **05**, 090 (2013). doi:10.1007/JHEP05(2013)090. arXiv:1303.4811
64. S.D. Ellis, C.K. Vermilion, J.R. Walsh, Techniques for improved heavy particle searches with jet substructure. Phys. Rev. D **80**, 051501 (2009). doi:10.1103/PhysRevD.80.051501. arXiv:0903.5081
65. S.D. Ellis, C.K. Vermilion, J.R. Walsh, Recombination algorithms and jet substructure: pruning as a tool for heavy particle searches. Phys. Rev. D **81**, 094023 (2010). doi:10.1103/PhysRevD.81.094023. arXiv:0912.0033
66. CMS Collaboration, Boosted top jet tagging at CMS. CMS Physics Analysis Summary CMS-PAS-JME-13-007 (2013)
67. M.J. Oreglia, A study of the reactions $\psi' \to \gamma\gamma\psi$. PhD thesis, Stanford University (1980). SLAC Report SLAC-R-236, see Appendix D
68. CMS Collaboration, Measurement of W^+W^- and ZZ production cross sections in pp collisions at $\sqrt{s} = 8$ TeV. Phys. Lett. B **721**, 190 (2013). doi:10.1016/j.physletb.2013.03.027. arXiv:1301.4698
69. CMS Collaboration, Measurements of inclusive W and Z cross sections in pp collisions at $\sqrt{s} = 7$ TeV. J. High Energy Phys. **01**, 080 (2011). doi:10.1007/JHEP01(2011)080
70. CMS Collaboration, Measurement of the inelastic proton-proton cross section at $\sqrt{s} = 7$ TeV. Phys. Lett. B **722**, 5 (2013). doi:10.1016/j.physletb.2013.03.024. arXiv:1210.6718
71. TOTEM Collaboration, Luminosity-independent measurement of the proton–proton total cross section at $\sqrt{s} = 8$ TeV. Phys. Rev. Lett. **111**, 012001. doi:10.1103/PhysRevLett.111.012001
72. M. Botje et al., The PDF4LHC working group interim recommendations (2011). arXiv:1101.0538
73. S. Alekhin et al., The PDF4LHC working group interim report (2011). arXiv:1101.0536

CMS Collaboration

Yerevan Physics Institute, Yerevan, Armenia
V. Khachatryan, A. M. Sirunyan, A. Tumasyan

Institut für Hochenergiephysik der OeAW, Vienna, Austria
W. Adam, E. Asilar, T. Bergauer, J. Brandstetter, E. Brondolin, M. Dragicevic, J. Erö, M. Flechl, M. Friedl, R. Frühwirth[1], V. M. Ghete, C. Hartl, N. Hörmann, J. Hrubec, M. Jeitler[1], V. Knünz, A. König, M. Krammer[1], I. Krätschmer, D. Liko, T. Matsushita, I. Mikulec, D. Rabady[2], B. Rahbaran, H. Rohringer, J. Schieck[1], R. Schöfbeck, J. Strauss, W. Treberer-Treberspurg, W. Waltenberger, C.-E. Wulz[1]

National Centre for Particle and High Energy Physics, Minsk, Belarus
V. Mossolov, N. Shumeiko, J. Suarez Gonzalez

Universiteit Antwerpen, Antwerp, Belgium
S. Alderweireldt, T. Cornelis, E. A. De Wolf, X. Janssen, A. Knutsson, J. Lauwers, S. Luyckx, M. Van De Klundert, H. Van Haevermaet, P. Van Mechelen, N. Van Remortel, A. Van Spilbeeck

Vrije Universiteit Brussel, Brussels, Belgium
S. Abu Zeid, F. Blekman, J. D'Hondt, N. Daci, I. De Bruyn, K. Deroover, N. Heracleous, J. Keaveney, S. Lowette, L. Moreels, A. Olbrechts, Q. Python, D. Strom, S. Tavernier, W. Van Doninck, P. Van Mulders, G. P. Van Onsem, I. Van Parijs

Université Libre de Bruxelles, Brussels, Belgium
P. Barria, H. Brun, C. Caillol, B. Clerbaux, G. De Lentdecker, G. Fasanella, L. Favart, A. Grebenyuk, G. Karapostoli, T. Lenzi, A. Léonard, T. Maerschalk, A. Marinov, L. Perniè, A. Randle-conde, T. Reis, T. Seva, C. Vander Velde, P. Vanlaer, R. Yonamine, F. Zenoni, F. Zhang[3]

Ghent University, Ghent, Belgium
K. Beernaert, L. Benucci, A. Cimmino, S. Crucy, D. Dobur, A. Fagot, G. Garcia, M. Gul, J. Mccartin, A. A. Ocampo Rios, D. Poyraz, D. Ryckbosch, S. Salva, M. Sigamani, M. Tytgat, W. Van Driessche, E. Yazgan, N. Zaganidis

Université Catholique de Louvain, Louvain-la-Neuve, Belgium
S. Basegmez, C. Beluffi[4], O. Bondu, S. Brochet, G. Bruno, A. Caudron, L. Ceard, G. G. Da Silveira, C. Delaere, D. Favart, L. Forthomme, A. Giammanco[5], J. Hollar, A. Jafari, P. Jez, M. Komm, V. Lemaitre, A. Mertens, M. Musich, C. Nuttens, L. Perrini, A. Pin, K. Piotrzkowski, A. Popov[6], L. Quertenmont, M. Selvaggi, M. Vidal Marono

Université de Mons, Mons, Belgium
N. Beliy, G. H. Hammad

Centro Brasileiro de Pesquisas Fisicas, Rio de Janeiro, Brazil
W. L. AldáJúnior, F. L. Alves, G. A. Alves, L. Brito, M. Correa Martins Junior, M. Hamer, C. Hensel, C. Mora Herrera, A. Moraes, M. E. Pol, P. Rebello Teles

Universidade do Estado do Rio de Janeiro, Rio de Janeiro, Brazil
E. Belchior Batista Das Chagas, W. Carvalho, J. Chinellato[7], A. Custódio, E. M. Da Costa, D. De Jesus Damiao, C. De Oliveira Martins, S. Fonseca De Souza, L.M. Huertas Guativa, H. Malbouisson, D. Matos Figueiredo, L. Mundim, H. Nogima, W. L. Prado Da Silva, A. Santoro, A. Sznajder, E. J. Tonelli Manganote[7], A. Vilela Pereira

Universidade Estadual Paulista[a], Universidade Federal do ABC[b], São Paulo, Brazil
S. Ahuja[a], C. A. Bernardes[b], A. De Souza Santos[b], S. Dogra[a], T. R. Fernandez Perez Tomei[a], E. M. Gregores[b], P. G. Mercadante[b], C.S. Moon[a,8], S. F. Novaes[a], Sandra S. Padula[a], D. Romero Abad, J.C. Ruiz Vargas

Institute for Nuclear Research and Nuclear Energy, Sofia, Bulgaria
A. Aleksandrov, R. Hadjiiska, P. Iaydjiev, M. Rodozov, S. Stoykova, G. Sultanov, M. Vutova

University of Sofia, Sofia, Bulgaria
A. Dimitrov, I. Glushkov, L. Litov, B. Pavlov, P. Petkov

Institute of High Energy Physics, Beijing, China
M. Ahmad, J. G. Bian, G. M. Chen, H. S. Chen, M. Chen, T. Cheng, R. Du, C. H. Jiang, R. Plestina[9], F. Romeo, S. M. Shaheen, A. Spiezia, J. Tao, C. Wang, Z. Wang, H. Zhang

State Key Laboratory of Nuclear Physics and Technology, Peking University, Beijing, China
C. Asawatangtrakuldee, Y. Ban, Q. Li, S. Liu, Y. Mao, S. J. Qian, D. Wang, M. Wang, Z. Xu

Universidad de Los Andes, Bogotá, Colombia
C. Avila, A. Cabrera, L. F. Chaparro Sierra, C. Florez, J. P. Gomez, B. Gomez Moreno, J. C. Sanabria

Faculty of Electrical Engineering, Mechanical Engineering and Naval Architecture, University of Split, Split, Croatia
N. Godinovic, D. Lelas, I. Puljak, P. M. Ribeiro Cipriano

Faculty of Science, University of Split, Split, Croatia
Z. Antunovic, M. Kovac

Institute Rudjer Boskovic, Zagreb, Croatia
V. Brigljevic, K. Kadija, J. Luetic, S. Micanovic, L. Sudic

University of Cyprus, Nicosia, Cyprus
A. Attikis, G. Mavromanolakis, J. Mousa, C. Nicolaou, F. Ptochos, P. A. Razis, H. Rykaczewski

Charles University, Prague, Czech Republic
M. Bodlak, M. Finger[10], M. Finger Jr.[10]

Academy of Scientific Research and Technology of the Arab Republic of Egypt, Egyptian Network of High Energy Physics, Cairo, Egypt
Y. Assran[11], S. Elgammal[12], A. Ellithi Kamel[13], M. A. Mahmoud[14]

National Institute of Chemical Physics and Biophysics, Tallinn, Estonia
B. Calpas, M. Kadastik, M. Murumaa, M. Raidal, A. Tiko, C. Veelken

Department of Physics, University of Helsinki, Helsinki, Finland
P. Eerola, J. Pekkanen, M. Voutilainen

Helsinki Institute of Physics, Helsinki, Finland
J. Härkönen, V. Karimäki, R. Kinnunen, T. Lampén, K. Lassila-Perini, S. Lehti, T. Lindén, P. Luukka, T. Mäenpää, T. Peltola, E. Tuominen, J. Tuominiemi, E. Tuovinen, L. Wendland

Lappeenranta University of Technology, Lappeenranta, Finland
J. Talvitie, T. Tuuva

DSM/IRFU, CEA/Saclay, Gif-sur-Yvette, France
M. Besancon, F. Couderc, M. Dejardin, D. Denegri, B. Fabbro, J. L. Faure, C. Favaro, F. Ferri, S. Ganjour, A. Givernaud, P. Gras, G. Hamel de Monchenault, P. Jarry, E. Locci, M. Machet, J. Malcles, J. Rander, A. Rosowsky, M. Titov, A. Zghiche

Laboratoire Leprince-Ringuet, Ecole Polytechnique, IN2P3-CNRS, Palaiseau, France
I. Antropov, S. Baffioni, F. Beaudette, P. Busson, L. Cadamuro, E. Chapon, C. Charlot, T. Dahms, O. Davignon, N. Filipovic, A. Florent, R. Granier de Cassagnac, S. Lisniak, L. Mastrolorenzo, P. Miné, I. N. Naranjo, M. Nguyen, C. Ochando, G. Ortona, P. Paganini, P. Pigard, S. Regnard, R. Salerno, J. B. Sauvan, Y. Sirois, T. Strebler, Y. Yilmaz, A. Zabi

Institut Pluridisciplinaire Hubert Curien, Université de Strasbourg, Université de Haute Alsace Mulhouse, CNRS/IN2P3, Strasbourg, France
J.-L. Agram[15], J. Andrea, A. Aubin, D. Bloch, J.-M. Brom, M. Buttignol, E. C. Chabert, N. Chanon, C. Collard, E. Conte[15], X. Coubez, J.-C. Fontaine[15], D. Gelé, U. Goerlach, C. Goetzmann, A.-C. Le Bihan, J. A. Merlin[2], K. Skovpen, P. Van Hove

Centre de Calcul de l'Institut National de Physique Nucleaire et de Physique des Particules, CNRS/IN2P3, Villeurbanne, France
S. Gadrat

Institut de Physique Nucléaire de Lyon, Université de Lyon, Université Claude Bernard Lyon 1, CNRS-IN2P3, Villeurbanne, France
S. Beauceron, C. Bernet, G. Boudoul, E. Bouvier, C. A. Carrillo Montoya, R. Chierici, D. Contardo, B. Courbon, P. Depasse, H. El Mamouni, J. Fan, J. Fay, S. Gascon, M. Gouzevitch, B. Ille, F. Lagarde, I. B. Laktineh, M. Lethuillier, L. Mirabito, A. L. Pequegnot, S. Perries, J. D. Ruiz Alvarez, D. Sabes, L. Sgandurra, V. Sordini, M. Vander Donckt, P. Verdier, S. Viret

Georgian Technical University, Tbilisi, Georgia
T. Toriashvili[16]

Tbilisi State University, Tbilisi, Georgia
L. Rurua

I. Physikalisches Institut, RWTH Aachen University, Aachen, Germany
C. Autermann, S. Beranek, M. Edelhoff, L. Feld, A. Heister, M. K. Kiesel, K. Klein, M. Lipinski, A. Ostapchuk, M. Preuten, F. Raupach, S. Schael, J. F. Schulte, T. Verlage, H. Weber, B. Wittmer, V. Zhukov[6]

III. Physikalisches Institut A, RWTH Aachen University, Aachen, Germany
M. Ata, M. Brodski, E. Dietz-Laursonn, D. Duchardt, M. Endres, M. Erdmann, S. Erdweg, T. Esch, R. Fischer, A. Güth, T. Hebbeker, C. Heidemann, K. Hoepfner, S. Knutzen, P. Kreuzer, M. Merschmeyer, A. Meyer, P. Millet, M. Olschewski, K. Padeken, P. Papacz, T. Pook, M. Radziej, H. Reithler, M. Rieger, F. Scheuch, L. Sonnenschein, D. Teyssier, S. Thüer

III. Physikalisches Institut B, RWTH Aachen University, Aachen, Germany
V. Cherepanov, Y. Erdogan, G. Flügge, H. Geenen, M. Geisler, F. Hoehle, B. Kargoll, T. Kress, Y. Kuessel, A. Künsken, J. Lingemann[2], A. Nehrkorn, A. Nowack, I. M. Nugent, C. Pistone, O. Pooth, A. Stahl

Deutsches Elektronen-Synchrotron, Hamburg, Germany
M. Aldaya Martin, I. Asin, N. Bartosik, O. Behnke, U. Behrens, A. J. Bell, K. Borras[17], A. Burgmeier, A. Campbell, S. Choudhury[18], F. Costanza, C. Diez Pardos, G. Dolinska, S. Dooling, T. Dorland, G. Eckerlin, D. Eckstein, T. Eichhorn, G. Flucke, E. Gallo[19], J. Garay Garcia, A. Geiser, A. Gizhko, P. Gunnellini, J. Hauk, M. Hempel[20], H. Jung, A. Kalogeropoulos, O. Karacheban[20], M. Kasemann, P. Katsas, J. Kieseler, C. Kleinwort, I. Korol, W. Lange, J. Leonard, K. Lipka, A. Lobanov, W. Lohmann[20], R. Mankel, I. Marfin[20], I.-A. Melzer-Pellmann, A. B. Meyer, G. Mittag, J. Mnich, A. Mussgiller, S. Naumann-Emme, A. Nayak, E. Ntomari, H. Perrey, D. Pitzl, R. Placakyte, A. Raspereza, B. Roland, M. Ö. Sahin, P. Saxena, T. Schoerner-Sadenius, M. Schröder, C. Seitz, S. Spannagel, K. D. Trippkewitz, R. Walsh, C. Wissing

University of Hamburg, Hamburg, Germany
V. Blobel, M. Centis Vignali, A. R. Draeger, J. Erfle, E. Garutti, K. Goebel, D. Gonzalez, M. Görner, J. Haller, M. Hoffmann, R. S. Höing, A. Junkes, R. Klanner, R. Kogler, N. Kovalchuk, T. Lapsien, T. Lenz, I. Marchesini, D. Marconi, M. Meyer, D. Nowatschin, J. Ott, F. Pantaleo[2], T. Peiffer, A. Perieanu, N. Pietsch, J. Poehlsen, D. Rathjens, C. Sander, C. Scharf, H. Schettler, P. Schleper, E. Schlieckau, A. Schmidt, J. Schwandt, V. Sola, H. Stadie, G. Steinbrück, H. Tholen, D. Troendle, E. Usai, L. Vanelderen, A. Vanhoefer, B. Vormwald

Institut für Experimentelle Kernphysik, Karlsruhe, Germany
M. Akbiyik, C. Barth, C. Baus, J. Berger, C. Böser, E. Butz, T. Chwalek, F. Colombo, W. De Boer, A. Descroix, A. Dierlamm, S. Fink, F. Frensch, R. Friese, M. Giffels, A. Gilbert, D. Haitz, F. Hartmann[2], S. M. Heindl, U. Husemann, I. Katkov[6], A. Kornmayer[2], P. Lobelle Pardo, B. Maier, H. Mildner, M. U. Mozer, T. Müller, Th. Müller, M. Plagge, G. Quast, K. Rabbertz, S. Röcker, F. Roscher, G. Sieber, H. J. Simonis, F. M. Stober, R. Ulrich, J. Wagner-Kuhr, S. Wayand, M. Weber, T. Weiler, C. Wöhrmann, R. Wolf

Institute of Nuclear and Particle Physics (INPP), NCSR Demokritos, Aghia Paraskevi, Greece
G. Anagnostou, G. Daskalakis, T. Geralis, V. A. Giakoumopoulou, A. Kyriakis, D. Loukas, A. Psallidas, I. Topsis-Giotis

National and Kapodistrian, University of Athens, Athens, Greece
A. Agapitos, S. Kesisoglou, A. Panagiotou, N. Saoulidou, E. Tziaferi

University of Ioánnina, Ioannina, Greece
I. Evangelou, G. Flouris, C. Foudas, P. Kokkas, N. Loukas, N. Manthos, I. Papadopoulos, E. Paradas, J. Strologas

Wigner Research Centre for Physics, Budapest, Hungary
G. Bencze, C. Hajdu, A. Hazi, P. Hidas, D. Horvath[21], F. Sikler, V. Veszpremi, G. Vesztergombi[22], A. J. Zsigmond

Institute of Nuclear Research ATOMKI, Debrecen, Hungary
N. Beni, S. Czellar, J. Karancsi[23], J. Molnar, Z. Szillasi

University of Debrecen, Debrecen, Hungary
M. Bartók[24], A. Makovec, P. Raics, Z. L. Trocsanyi, B. Ujvari

National Institute of Science Education and Research, Bhubaneswar, India
P. Mal, K. Mandal, D. K. Sahoo, N. Sahoo, S. K. Swain

Panjab University, Chandigarh, India
S. Bansal, S. B. Beri, V. Bhatnagar, R. Chawla, R. Gupta, U. Bhawandeep, A. K. Kalsi, A. Kaur, M. Kaur, R. Kumar, A. Mehta, M. Mittal, J. B. Singh, G. Walia

University of Delhi, Delhi, India
Ashok Kumar, A. Bhardwaj, B. C. Choudhary, R. B. Garg, A. Kumar, S. Malhotra, M. Naimuddin, N. Nishu, K. Ranjan, R. Sharma, V. Sharma

Saha Institute of Nuclear Physics, Kolkata, India
S. Bhattacharya, K. Chatterjee, S. Dey, S. Dutta, Sa. Jain, N. Majumdar, A. Modak, K. Mondal, S. Mukherjee, S. Mukhopadhyay, A. Roy, D. Roy, S. Roy Chowdhury, S. Sarkar, M. Sharan

Bhabha Atomic Research Centre, Mumbai, India
A. Abdulsalam, R. Chudasama, D. Dutta, V. Jha, V. Kumar, A. K. Mohanty[2], L. M. Pant, P. Shukla, A. Topkar

Tata Institute of Fundamental Research, Mumbai, India
T. Aziz, S. Banerjee, S. Bhowmik[25], R. M. Chatterjee, R. K. Dewanjee, S. Dugad, S. Ganguly, S. Ghosh, M. Guchait, A. Gurtu[26], G. Kole, S. Kumar, B. Mahakud, M. Maity[25], G. Majumder, K. Mazumdar, S. Mitra, G. B. Mohanty, B. Parida, T. Sarkar[25], N. Sur, B. Sutar, N. Wickramage[27]

Indian Institute of Science Education and Research (IISER), Pune, India
S. Chauhan, S. Dube, K. Kothekar, S. Sharma

Institute for Research in Fundamental Sciences (IPM), Tehran, Iran
H. Bakhshiansohi, H. Behnamian, S. M. Etesami[28], A. Fahim[29], R. Goldouzian, M. Khakzad, M. Mohammadi Najafabadi, M. Naseri, S. Paktinat Mehdiabadi, F. Rezaei Hosseinabadi, B. Safarzadeh[30], M. Zeinali

University College Dublin, Dublin, Ireland
M. Felcini, M. Grunewald

INFN Sezione di Bari[a], Università di Bari[b], Politecnico di Bari[c], Bari, Italy
M. Abbrescia[a,b], C. Calabria[a,b], C. Caputo[a,b], A. Colaleo[a], D. Creanza[a,c], L. Cristella[a,b], N. De Filippis[a,c], M. De Palma[a,b], L. Fiore[a], G. Iaselli[a,c], G. Maggi[a,c], M. Maggi[a], G. Miniello[a,b], S. My[a,c], S. Nuzzo[a,b], A. Pompili[a,b], G. Pugliese[a,c], R. Radogna[a,b,], A. Ranieri[a], G. Selvaggi[a,b], L. Silvestris[a,2], R. Venditti[a,b], P. Verwilligen[a]

INFN Sezione di Bologna[a], Università di Bologna[b], Bologna, Italy
G. Abbiendi[a], C. Battilana[2], A. C. Benvenuti[a], D. Bonacorsi[a,b], S. Braibant-Giacomelli[a,b], L. Brigliadori[a,b], R. Campanini[a,b], P. Capiluppi[a,b], A. Castro[a,b], F. R. Cavallo[a], S. S. Chhibra[a,b], G. Codispoti[a,b], M. Cuffiani[a,b], G. M. Dallavalle[a], F. Fabbri[a], A. Fanfani[a,b], D. Fasanella[a,b], P. Giacomelli[a], C. Grandi[a], L. Guiducci[a,b], S. Marcellini[a], G. Masetti[a], A. Montanari[a], F. L. Navarria[a,b], A. Perrotta[a], A. M. Rossi[a,b], T. Rovelli[a,b], G. P. Siroli[a,b], N. Tosi[a,b], R. Travaglini[a,b]

INFN Sezione di Catania[a], Università di Catania[b], Catania, Italy
G. Cappello[a], M. Chiorboli[a,b], S. Costa[a,b], A. Di Mattia[a], F. Giordano[a,b], R. Potenza[a,b], A. Tricomi[a,b], C. Tuve[a,b]

INFN Sezione di Firenze[a], Università di Firenze[b], Florence, Italy
G. Barbagli[a], V. Ciulli[a,b], C. Civinini[a], R. D'Alessandro[a,b], E. Focardi[a,b], S. Gonzi[a,b], V. Gori[a,b], P. Lenzi[a,b], M. Meschini[a], S. Paoletti[a], G. Sguazzoni[a], A. Tropiano[a,b], L. Viliani[a,b,2]

INFN Laboratori Nazionali di Frascati, Frascati, Italy
L. Benussi, S. Bianco, F. Fabbri, D. Piccolo, F. Primavera

INFN Sezione di Genova[a], Università di Genova[b], Genoa, Italy
V. Calvelli[a,b], F. Ferro[a], M. Lo Vetere[a,b], M. R. Monge[a,b], E. Robutti[a], S. Tosi[a,b]

INFN Sezione di Milano-Bicocca[a], Università di Milano-Bicocca[b], Milan, Italy
L. Brianza, M. E. Dinardo[a,b], S. Fiorendi[a,b], S. Gennai[a], R. Gerosa[a,b], A. Ghezzi[a,b], P. Govoni[a,b], S. Malvezzi[a], R. A. Manzoni[a,b], B. Marzocchi[a,b,2], D. Menasce[a], L. Moroni[a], M. Paganoni[a,b], D. Pedrini[a], S. Ragazzi[a,b], N. Redaelli[a], T. Tabarelli de Fatis[a,b]

INFN Sezione di Napoli[a], Università di Napoli 'Federico II'[b], Napoli, Italy, Università della Basilicata[c], Potenza, Italy, Università G. Marconi[d], Rome, Italy
S. Buontempo[a], N. Cavallo[a,c], S. Di Guida[a,d,2], M. Esposito[a,b], F. Fabozzi[a,c], A. O. M. Iorio[a,b], G. Lanza[a], L. Lista[a], S. Meola[a,d,2], M. Merola[a], P. Paolucci[a,2], C. Sciacca[a,b], F. Thyssen

INFN Sezione di Padova[a], Università di Padova[b], Padova, Italy, Università di Trento[c], Trento, Italy
P. Azzi[a,2], N. Bacchetta[a], L. Benato[a,b], D. Bisello[a,b], A. Boletti[a,b], R. Branca[a,b], R. Carlin[a,b], A. Carvalho Antunes De Oliveira[a,b], P. Checchia[a], M. Dall'Osso[a,b,2], T. Dorigo[a], U. Dosselli[a], F. Gasparini[a,b], U. Gasparini[a,b], A. Gozzelino[a], K. Kanishchev[a,c], S. Lacaprara[a], M. Margoni[a,b], A. T. Meneguzzo[a,b], J. Pazzini[a,b], N. Pozzobon[a,b], P. Ronchese[a,b], F. Simonetto[a,b], E. Torassa [a], M. Tosi[a,b], M. Zanetti, P. Zotto[a,b], A. Zucchetta[a,b,2], G. Zumerle[a,b,]

INFN Sezione di Pavia[a], Università di Pavia[b], Pavia, Italy
A. Braghieri[a], A. Magnani[a], P. Montagna[a,b], S. P. Ratti[a,b], V. Re[a], C. Riccardi[a,b], P. Salvini[a], I. Vai[a], P. Vitulo[a,b]

INFN Sezione di Perugia[a], Università di Perugia[b], Perugia, Italy
L. Alunni Solestizi[a,b], M. Biasini[a,b], G. M. Bilei[a], D. Ciangottini[a,b,2], L. Fanò[a,b], P. Lariccia[a,b], G. Mantovani[a,b], M. Menichelli[a], A. Saha[a], A. Santocchia[a,b]

INFN Sezione di Pisa[a], Università di Pisa[b], Scuola Normale Superiore di Pisa[c], Pisa, Italy
K. Androsov[a,31], P. Azzurri[a], G. Bagliesi[a], J. Bernardini[a], T. Boccali[a], R. Castaldi[a], M. A. Ciocci[a,31], R. Dell'Orso[a], S. Donato[a,c,2], G. Fedi, L. Foà[a,c,†], A. Giassi[a], M. T. Grippo[a,31], F. Ligabue[a,c], T. Lomtadze[a], L. Martini[a,b], A. Messineo[a,b], F. Palla[a], A. Rizzi[a,b], A. Savoy-Navarro[a,32], A. T. Serban[a], P. Spagnolo[a], R. Tenchini[a], G. Tonelli[a,b], A. Venturi[a], P. G. Verdini[a]

INFN Sezione di Roma[a], Università di Roma[b], Rome, Italy
L. Barone[a,b], F. Cavallari[a], G. D'imperio[a,b,2], D. Del Re[a,b], M. Diemoz[a], S. Gelli[a,b], C. Jorda[a], E. Longo[a,b], F. Margaroli[a,b], P. Meridiani[a], G. Organtini[a,b], R. Paramatti[a], F. Preiato[a,b], S. Rahatlou[a,b], C. Rovelli[a], F. Santanastasio[a,b], P. Traczyk[a,b,2]

INFN Sezione di Torino[a], Università di Torino[b], Turin, Italy, Università del Piemonte Orientale[c], Novara, Italy
N. Amapane[a,b], R. Arcidiacono[a,c,2], S. Argiro[a,b], M. Arneodo[a,c], R. Bellan[a,b], C. Biino[a], N. Cartiglia[a], M. Costa[a,b], R. Covarelli[a,b], A. Degano[a,b], N. Demaria[a], L. Finco[a,b,2], B. Kiani[a,b], C. Mariotti[a], S. Maselli[a], E. Migliore[a,b], V. Monaco[a,b], E. Monteil[a,b], M. M. Obertino[a,b], L. Pacher[a,b], N. Pastrone[a], M. Pelliccioni[a], G. L. Pinna Angioni[a,b], F. Ravera[a,b], A. Romero[a,b], M. Ruspa[a,c], R. Sacchi[a,b], A. Solano[a,b], A. Staiano[a], U. Tamponi[a]

INFN Sezione di Trieste[a], Università di Trieste[b], Trieste, Italy
S. Belforte[a], V. Candelise[a,b,2], M. Casarsa[a], F. Cossutti[a], G. Della Ricca[a,b], B. Gobbo[a], C. La Licata[a,b], M. Marone[a,b], A. Schizzi[a,b], A. Zanetti[a]

Kangwon National University, Chunchon, Korea
A. Kropivnitskaya, S. K. Nam

Kyungpook National University, Daegu, Korea
D. H. Kim, G. N. Kim, M. S. Kim, D. J. Kong, S. Lee, Y. D. Oh, A. Sakharov, D. C. Son

Chonbuk National University, Jeonju, Korea
J. A. Brochero Cifuentes, H. Kim, T. J. Kim

Institute for Universe and Elementary Particles, Chonnam National University, Kwangju, Korea
S. Song

Korea University, Seoul, Korea
S. Choi, Y. Go, D. Gyun, B. Hong, M. Jo, H. Kim, Y. Kim, B. Lee, K. Lee, K. S. Lee, S. Lee, S. K. Park, Y. Roh

Seoul National University, Seoul, Korea
H. D. Yoo

University of Seoul, Seoul, Korea
M. Choi, H. Kim, J. H. Kim, J. S. H. Lee, I. C. Park, G. Ryu, M. S. Ryu

Sungkyunkwan University, Suwon, Korea
Y. Choi, J. Goh, D. Kim, E. Kwon, J. Lee, I. Yu

Vilnius University, Vilnius, Lithuania
V. Dudenas, A. Juodagalvis, J. Vaitkus

National Centre for Particle Physics, Universiti Malaya, Kuala Lumpur, Malaysia
I. Ahmed, Z. A. Ibrahim, J. R. Komaragiri, M. A. B. Md Ali[33], F. Mohamad Idris[34], W. A. T. Wan Abdullah, M. N. Yusli

Centro de Investigacion y de Estudios Avanzados del IPN, Mexico City, Mexico
E. Casimiro Linares, H. Castilla-Valdez, E. De La Cruz-Burelo, I. Heredia-De La Cruz[35], A. Hernandez-Almada, R. Lopez-Fernandez, A. Sanchez-Hernandez

Universidad Iberoamericana, Mexico City, Mexico
S. Carrillo Moreno, F. Vazquez Valencia

Benemerita Universidad Autonoma de Puebla, Puebla, Mexico
I. Pedraza, H. A. Salazar Ibarguen

Universidad Autónoma de San Luis Potosí, San Luis Potosí, Mexico
A. Morelos Pineda

University of Auckland, Auckland, New Zealand
D. Krofcheck

University of Canterbury, Christchurch, New Zealand
P. H. Butler

National Centre for Physics, Quaid-I-Azam University, Islamabad, Pakistan
A. Ahmad, M. Ahmad, Q. Hassan, H. R. Hoorani, W. A. Khan, T. Khurshid, M. Shoaib

National Centre for Nuclear Research, Swierk, Poland
H. Bialkowska, M. Bluj, B. Boimska, T. Frueboes, M. Górski, M. Kazana, K. Nawrocki, K. Romanowska-Rybinska, M. Szleper, P. Zalewski

Institute of Experimental Physics, Faculty of Physics, University of Warsaw, Warsaw, Poland
G. Brona, K. Bunkowski, A. Byszuk[36], K. Doroba, A. Kalinowski, M. Konecki, J. Krolikowski, M. Misiura, M. Olszewski, M. Walczak

Laboratório de Instrumentação e Física Experimental de Partículas, Lisbon, Portugal
P. Bargassa, C. Beirão Da Cruz E Silva, A. Di Francesco, P. Faccioli, P. G. Ferreira Parracho, M. Gallinaro, N. Leonardo, L. Lloret Iglesias, F. Nguyen, J. Rodrigues Antunes, J. Seixas, O. Toldaiev, D. Vadruccio, J. Varela, P. Vischia

Joint Institute for Nuclear Research, Dubna, Russia
S. Afanasiev, P. Bunin, M. Gavrilenko, I. Golutvin, I. Gorbunov, A. Kamenev, V. Karjavin, V. Konoplyanikov, A. Lanev, A. Malakhov, V. Matveev[37,38], P. Moisenz, V. Palichik, V. Perelygin, S. Shmatov, S. Shulha, N. Skatchkov, V. Smirnov, A. Zarubin

Petersburg Nuclear Physics Institute, Gatchina, St. Petersburg, Russia
V. Golovtsov, Y. Ivanov, V. Kim[39], E. Kuznetsova, P. Levchenko, V. Murzin, V. Oreshkin, I. Smirnov, V. Sulimov, L. Uvarov, S. Vavilov, A. Vorobyev

Institute for Nuclear Research, Moscow, Russia
Yu. Andreev, A. Dermenev, S. Gninenko, N. Golubev, A. Karneyeu, M. Kirsanov, N. Krasnikov, A. Pashenkov, D. Tlisov, A. Toropin

Institute for Theoretical and Experimental Physics, Moscow, Russia
V. Epshteyn, V. Gavrilov, N. Lychkovskaya, V. Popov, I. Pozdnyakov, G. Safronov, A. Spiridonov, E. Vlasov, A. Zhokin

National Research Nuclear University 'Moscow Engineering Physics Institute' (MEPhI), Moscow, Russia
A. Bylinkin

P. N. Lebedev Physical Institute, Moscow, Russia
V. Andreev, M. Azarkin[38], I. Dremin[38], M. Kirakosyan, A. Leonidov[38], G. Mesyats, S. V. Rusakov

Skobeltsyn Institute of Nuclear Physics, Lomonosov Moscow State University, Moscow, Russia
A. Baskakov, A. Belyaev, E. Boos, V. Bunichev, M. Dubinin[40], L. Dudko, A. Ershov, A. Gribushin, V. Klyukhin, O. Kodolova, I. Lokhtin, I. Myagkov, S. Obraztsov, V. Savrin, A Snigirev

State Research Center of Russian Federation, Institute for High Energy Physics, Protvino, Russia
I. Azhgirey, I. Bayshev, S. Bitioukov, V. Kachanov, A. Kalinin, D. Konstantinov, V. Krychkine, V. Petrov, R. Ryutin, A. Sobol, L. Tourtchanovitch, S. Troshin, N. Tyurin, A. Uzunian, A. Volkov

Faculty of Physics and Vinca Institute of Nuclear Sciences, University of Belgrade, Belgrade, Serbia
P. Adzic[41], J. Milosevic, V. Rekovic

Centro de Investigaciones Energéticas Medioambientales y Tecnológicas (CIEMAT), Madrid, Spain
J. Alcaraz Maestre, E. Calvo, M. Cerrada, M. Chamizo Llatas, N. Colino, B. De La Cruz, A. Delgado Peris, D. Domínguez Vázquez, A. Escalante Del Valle, C. Fernandez Bedoya, J. P. Fernández Ramos, J. Flix, M. C. Fouz, P. Garcia-Abia, O. Gonzalez Lopez, S. Goy Lopez, J. M. Hernandez, M. I. Josa, E. Navarro De Martino, A. Pérez-Calero Yzquierdo, J. Puerta Pelayo, A. Quintario Olmeda, I. Redondo, L. Romero, J. Santaolalla, M. S. Soares

Universidad Autónoma de Madrid, Madrid, Spain
C. Albajar, J. F. de Trocóniz, M. Missiroli, D. Moran

Universidad de Oviedo, Oviedo, Spain
J. Cuevas, J. Fernandez Menendez, S. Folgueras, I. Gonzalez Caballero, E. Palencia Cortezon, J. M. Vizan Garcia

Instituto de Física de Cantabria (IFCA), CSIC-Universidad de Cantabria, Santander, Spain
I. J. Cabrillo, A. Calderon, J. R. Castiñeiras De Saa, P. De Castro Manzano, J. Duarte Campderros, M. Fernandez, J. Garcia-Ferrero, G. Gomez, A. Lopez Virto, J. Marco, R. Marco, C. Martinez Rivero, F. Matorras, F. J. Munoz Sanchez, J. Piedra Gomez, T. Rodrigo, A. Y. Rodríguez-Marrero, A. Ruiz-Jimeno, L. Scodellaro, N. Trevisani, I. Vila, R. Vilar Cortabitarte

CERN, European Organization for Nuclear Research, Geneva, Switzerland
D. Abbaneo, E. Auffray, G. Auzinger, M. Bachtis, P. Baillon, A. H. Ball, D. Barney, A. Benaglia, J. Bendavid, L. Benhabib, J. F. Benitez, G. M. Berruti, P. Bloch, A. Bocci, A. Bonato, C. Botta, H. Breuker, T. Camporesi, R. Castello, G. Cerminara, M. D'Alfonso, D. d'Enterria, A. Dabrowski, V. Daponte, A. David, M. De Gruttola, F. De Guio, A. De Roeck, S. De Visscher, E. Di Marco, M. Dobson, M. Dordevic, B. Dorney, T. du Pree, M. Dünser, N. Dupont, A. Elliott-Peisert, G. Franzoni, W. Funk, D. Gigi, K. Gill, D. Giordano, M. Girone, F. Glege, R. Guida, S. Gundacker, M. Guthoff, J. Hammer, P. Harris, J. Hegeman, V. Innocente, P. Janot, H. Kirschenmann, M. J. Kortelainen, K. Kousouris, K. Krajczar, P. Lecoq, C. Lourenço, M. T. Lucchini, N. Magini, L. Malgeri, M. Mannelli, A. Martelli, L. Masetti, F. Meijers, S. Mersi, E. Meschi, F. Moortgat, S. Morovic, M. Mulders, M. V. Nemallapudi, H. Neugebauer, S. Orfanelli[42], L. Orsini, L. Pape, E. Perez, M. Peruzzi, A. Petrilli, G. Petrucciani, A. Pfeiffer, D. Piparo, A. Racz, G. Rolandi[43], M. Rovere, M. Ruan, H. Sakulin, C. Schäfer, C. Schwick, M Seidel, A. Sharma, P. Silva, M. Simon, P. Sphicas[44], J. Steggemann, B. Stieger, M. Stoye, Y. Takahashi, D. Treille, A. Triossi, A. Tsirou, G. I. Veres[22], N. Wardle, H. K. Wöhri, A. Zagozdzinska[36], W. D. Zeuner

Paul Scherrer Institut, Villigen, Switzerland
W. Bertl, K. Deiters, W. Erdmann, R. Horisberger, Q. Ingram, H. C. Kaestli, D. Kotlinski, U. Langenegger, D. Renker, T. Rohe

Institute for Particle Physics, ETH Zurich, Zurich, Switzerland
F. Bachmair, L. Bäni, L. Bianchini, B. Casal, G. Dissertori, M. Dittmar, M. Donegà, P. Eller, C. Grab, C. Heidegger, D. Hits, J. Hoss, G. Kasieczka, W. Lustermann, B. Mangano, M. Marionneau, P. Martinez Ruiz del Arbol, M. Masciovecchio, D. Meister, F. Micheli, P. Musella, F. Nessi-Tedaldi, F. Pandolfi, J. Pata, F. Pauss, L. Perrozzi, M. Quittnat, M. Rossini, A. Starodumov[45], M. Takahashi, V. R. Tavolaro, K. Theofilatos, R. Wallny

Universität Zürich, Zurich, Switzerland
T. K. Aarrestad, C. Amsler[46], L. Caminada, M. F. Canelli, V. Chiochia, A. De Cosa, C. Galloni, A. Hinzmann, T. Hreus, B. Kilminster, C. Lange, J. Ngadiuba, D. Pinna, P. Robmann, F. J. Ronga, D. Salerno, Y. Yang

National Central University, Chung-Li, Taiwan
M. Cardaci, K. H. Chen, T. H. Doan, Sh. Jain, R. Khurana, M. Konyushikhin, C. M. Kuo, W. Lin, Y. J. Lu, S. S. Yu

National Taiwan University (NTU), Taipei, Taiwan
Arun Kumar, R. Bartek, P. Chang, Y. H. Chang, Y. W. Chang, Y. Chao, K. F. Chen, P. H. Chen, C. Dietz, F. Fiori, U. Grundler, W.-S. Hou, Y. Hsiung, Y. F. Liu, R.-S. Lu, M. Miñano Moya, E. Petrakou, J. f. Tsai, Y. M. Tzeng

Department of Physics, Faculty of Science, Chulalongkorn University, Bangkok, Thailand
B. Asavapibhop, K. Kovitanggoon, G. Singh, N. Srimanobhas, N. Suwonjandee

Cukurova University, Adana, Turkey
A. Adiguzel, M. N. Bakirci[47], S. Cerci[48], Z. S. Demiroglu, C. Dozen, I. Dumanoglu, E. Eskut, S. Girgis, G. Gokbulut, Y. Guler, E. Gurpinar, I. Hos, E. E. Kangal[49], A. Kayis Topaksu, G. Onengut[50], K. Ozdemir[51], A. Polatoz, M. Vergili, C. Zorbilmez

Physics Department, Middle East Technical University, Ankara, Turkey
I. V. Akin, B. Bilin, S. Bilmis, B. Isildak[52], G. Karapinar[53], M. Yalvac, M. Zeyrek

Bogazici University, Istanbul, Turkey
E. Gülmez, M. Kaya[54], O. Kaya[55], E. A. Yetkin[56], T. Yetkin[57]

Istanbul Technical University, Istanbul, Turkey
A. Cakir, K. Cankocak, S.Sen[58], F. I. Vardarlı

Institute for Scintillation Materials of National Academy of Science of Ukraine, Kharkov, Ukraine
B. Grynyov

National Scientific Center, Kharkov Institute of Physics and Technology, Kharkov, Ukraine
L. Levchuk, P. Sorokin

University of Bristol, Bristol, UK
R. Aggleton, F. Ball, L. Beck, J. J. Brooke, E. Clement, D. Cussans, H. Flacher, J. Goldstein, M. Grimes, G. P. Heath, H. F. Heath, J. Jacob, L. Kreczko, C. Lucas, Z. Meng, D. M. Newbold[59], S. Paramesvaran, A. Poll, T. Sakuma, S. Seif El Nasr-storey, S. Senkin, D. Smith, V. J. Smith

Rutherford Appleton Laboratory, Didcot, UK
K. W. Bell, A. Belyaev[60], C. Brew, R. M. Brown, L. Calligaris, D. Cieri, D. J. A. Cockerill, J. A. Coughlan, K. Harder, S. Harper, E. Olaiya, D. Petyt, C. H. Shepherd-Themistocleous, A. Thea, I. R. Tomalin, T. Williams, W. J. Womersley, S. D. Worm

Imperial College, London, UK
M. Baber, R. Bainbridge, O. Buchmuller, A. Bundock, D. Burton, S. Casasso, M. Citron, D. Colling, L. Corpe, N. Cripps, P. Dauncey, G. Davies, A. De Wit, M. Della Negra, P. Dunne, A. Elwood, W. Ferguson, J. Fulcher, D. Futyan, G. Hall, G. Iles, M. Kenzie, R. Lane, R. Lucas[59], L. Lyons, A.-M. Magnan, S. Malik, J. Nash, A. Nikitenko[45], J. Pela, M. Pesaresi, K. Petridis, D. M. Raymond, A. Richards, A. Rose, C. Seez, A. Tapper, K. Uchida, M. Vazquez Acosta[61], T. Virdee, S. C. Zenz

Brunel University, Uxbridge, UK
J. E. Cole, P. R. Hobson, A. Khan, P. Kyberd, D. Leggat, D. Leslie, I. D. Reid, P. Symonds, L. Teodorescu, M. Turner

Baylor University, Waco, USA
A. Borzou, K. Call, J. Dittmann, K. Hatakeyama, H. Liu, N. Pastika

The University of Alabama, Tuscaloosa, USA
O. Charaf, S. I. Cooper, C. Henderson, P. Rumerio

Boston University, Boston, USA
D. Arcaro, A. Avetisyan, T. Bose, C. Fantasia, D. Gastler, P. Lawson, D. Rankin, C. Richardson, J. Rohlf, J. St. John, L. Sulak, D. Zou

Brown University, Providence, USA
J. Alimena, E. Berry, S. Bhattacharya, D. Cutts, N. Dhingra, A. Ferapontov, A. Garabedian, J. Hakala, U. Heintz, E. Laird, G. Landsberg, Z. Mao, M. Narain, S. Piperov, S. Sagir, R. Syarif

University of California, Davis, Davis, USA
R. Breedon, G. Breto, M. Calderon De La Barca Sanchez, S. Chauhan, M. Chertok, J. Conway, R. Conway, P. T. Cox, R. Erbacher, M. Gardner, W. Ko, R. Lander, M. Mulhearn, D. Pellett, J. Pilot, F. Ricci-Tam, S. Shalhout, J. Smith, M. Squires, D. Stolp, M. Tripathi, S. Wilbur, R. Yohay

University of California, Los Angeles, USA
R. Cousins, P. Everaerts, C. Farrell, J. Hauser, M. Ignatenko, D. Saltzberg, E. Takasugi, V. Valuev, M. Weber

University of California, Riverside, Riverside, USA
K. Burt, R. Clare, J. Ellison, J. W. Gary, G. Hanson, J. Heilman, M. Ivova PANEVA, P. Jandir, E. Kennedy, F. Lacroix, O. R. Long, A. Luthra, M. Malberti, M. Olmedo Negrete, A. Shrinivas, H. Wei, S. Wimpenny, B. R. Yates

University of California, San Diego, La Jolla, USA
J. G. Branson, G. B. Cerati, S. Cittolin, R. T. D'Agnolo, M Derdzinski, A. Holzner, R. Kelley, D. Klein, J. Letts, I. Macneill, D. Olivito, S. Padhi, M. Pieri, M. Sani, V. Sharma, S. Simon, M. Tadel, A. Vartak, S. Wasserbaech[62], C. Welke, F. Würthwein, A. Yagil, G. Zevi Della Porta

University of California, Santa Barbara, Santa Barbara, USA
J. Bradmiller-Feld, C. Campagnari, A. Dishaw, V. Dutta, K. Flowers, M. Franco Sevilla, P. Geffert, C. George, F. Golf, L. Gouskos, J. Gran, J. Incandela, N. Mccoll, S. D. Mullin, J. Richman, D. Stuart, I. Suarez, C. West, J. Yoo

California Institute of Technology, Pasadena, USA
D. Anderson, A. Apresyan, A. Bornheim, J. Bunn, Y. Chen, J. Duarte, A. Mott, H. B. Newman, C. Pena, M. Pierini, M. Spiropulu, J. R. Vlimant, S. Xie, R. Y. Zhu

Carnegie Mellon University, Pittsburgh, USA
M. B. Andrews, V. Azzolini, A. Calamba, B. Carlson, T. Ferguson, M. Paulini, J. Russ, M. Sun, H. Vogel, I. Vorobiev

University of Colorado Boulder, Boulder, USA
J. P. Cumalat, W. T. Ford, A. Gaz, F. Jensen, A. Johnson, M. Krohn, T. Mulholland, U. Nauenberg, K. Stenson, S. R. Wagner

Cornell University, Ithaca, USA
J. Alexander, A. Chatterjee, J. Chaves, J. Chu, S. Dittmer, N. Eggert, N. Mirman, G. Nicolas Kaufman, J. R. Patterson, A. Rinkevicius, A. Ryd, L. Skinnari, L. Soffi, W. Sun, S. M. Tan, W. D. Teo, J. Thom, J. Thompson, J. Tucker, Y. Weng, P. Wittich

Fermi National Accelerator Laboratory, Batavia, USA
S. Abdullin, M. Albrow, J. Anderson, G. Apollinari, S. Banerjee, L. A. T. Bauerdick, A. Beretvas, J. Berryhill, P. C. Bhat, G. Bolla, K. Burkett, J. N. Butler, H. W. K. Cheung, F. Chlebana, S. Cihangir, V. D. Elvira, I. Fisk, J. Freeman, E. Gottschalk, L. Gray, D. Green, S. Grünendahl, O. Gutsche, J. Hanlon, D. Hare, R. M. Harris, S. Hasegawa, J. Hirschauer, Z. Hu, B. Jayatilaka, S. Jindariani, M. Johnson, U. Joshi, A. W. Jung, B. Klima, B. Kreis, S. Kwan[†], S. Lammel, J. Linacre, D. Lincoln, R. Lipton, T. Liu, R. Lopes De Sá, J. Lykken, K. Maeshima, J. M. Marraffino, V. I. Martinez Outschoorn,

S. Maruyama, D. Mason, P. McBride, P. Merkel, K. Mishra, S. Mrenna, S. Nahn, C. Newman-Holmes, V. O'Dell, K. Pedro, O. Prokofyev, G. Rakness, E. Sexton-Kennedy, A. Soha, W. J. Spalding, L. Spiegel, N. Strobbe, L. Taylor, S. Tkaczyk, N. V. Tran, L. Uplegger, E. W. Vaandering, C. Vernieri, M. Verzocchi, R. Vidal, H. A. Weber, A. Whitbeck, F. Yang

University of Florida, Gainesville, USA
D. Acosta, P. Avery, P. Bortignon, D. Bourilkov, A. Carnes, M. Carver, D. Curry, S. Das, R. D. Field, I. K. Furic, S. V. Gleyzer, J. Hugon, J. Konigsberg, A. Korytov, J. F. Low, P. Ma, K. Matchev, H. Mei, P. Milenovic[63], G. Mitselmakher, D. Rank, R. Rossin, L. Shchutska, M. Snowball, D. Sperka, N. Terentyev, L. Thomas, J. Wang, S. Wang, J. Yelton

Florida International University, Miami, USA
S. Hewamanage, S. Linn, P. Markowitz, G. Martinez, J. L. Rodriguez

Florida State University, Tallahassee, USA
A. Ackert, J. R. Adams, T. Adams, A. Askew, J. Bochenek, B. Diamond, J. Haas, S. Hagopian, V. Hagopian, K. F. Johnson, A. Khatiwada, H. Prosper, M. Weinberg

Florida Institute of Technology, Melbourne, USA
M. M. Baarmand, V. Bhopatkar, S. Colafranceschi, M. Hohlmann, H. Kalakhety, D. Noonan, T. Roy, F. Yumiceva

University of Illinois at Chicago (UIC), Chicago, USA
M. R. Adams, L. Apanasevich, D. Berry, R. R. Betts, I. Bucinskaite, R. Cavanaugh, O. Evdokimov, L. Gauthier, C. E. Gerber, D. J. Hofman, P. Kurt, C. O'Brien, I. D. Sandoval Gonzalez, C. Silkworth, P. Turner, N. Varelas, Z. Wu, M. Zakaria

The University of Iowa, Iowa City, USA
B. Bilki[65], W. Clarida, K. Dilsiz, S. Durgut, R. P. Gandrajula, M. Haytmyradov, V. Khristenko, J.-P. Merlo, H. Mermerkaya[66], A. Mestvirishvili, A. Moeller, J. Nachtman, H. Ogul, Y. Onel, F. Ozok[56], A. Penzo, C. Snyder, E. Tiras, J. Wetzel, K. Yi

Johns Hopkins University, Baltimore, USA
I. Anderson, B. A. Barnett, B. Blumenfeld, N. Eminizer, D. Fehling, L. Feng, A. V. Gritsan, P. Maksimovic, C. Martin, M. Osherson, J. Roskes, A. Sady, U. Sarica, M. Swartz, M. Xiao, Y. Xin, C. You

The University of Kansas, Lawrence, USA
P. Baringer, A. Bean, G. Benelli, C. Bruner, R. P. KennyIII, D. Majumder, M. Malek, M. Murray, S. Sanders, R. Stringer, Q. Wang

Kansas State University, Manhattan, USA
A. Ivanov, K. Kaadze, S. Khalil, M. Makouski, Y. Maravin, A. Mohammadi, L. K. Saini, N. Skhirtladze, S. Toda

Lawrence Livermore National Laboratory, Livermore, USA
D. Lange, F. Rebassoo, D. Wright

University of Maryland, College Park, USA
C. Anelli, A. Baden, O. Baron, A. Belloni, B. Calvert, S. C. Eno, C. Ferraioli, J. A. Gomez, N. J. Hadley, S. Jabeen, R. G. Kellogg, T. Kolberg, J. Kunkle, Y. Lu, A. C. Mignerey, Y. H. Shin, A. Skuja, M. B. Tonjes, S. C. Tonwar

Massachusetts Institute of Technology, Cambridge, USA
A. Apyan, R. Barbieri, A. Baty, K. Bierwagen, S. Brandt, W. Busza, I. A. Cali, Z. Demiragli, L. Di Matteo, G. Gomez Ceballos, M. Goncharov, D. Gulhan, Y. Iiyama, G. M. Innocenti, M. Klute, D. Kovalskyi, Y. S. Lai, Y.-J. Lee, A. Levin, P. D. Luckey, A. C. Marini, C. Mcginn, C. Mironov, S. Narayanan, X. Niu, C. Paus, D. Ralph, C. Roland, G. Roland, J. Salfeld-Nebgen, G. S. F. Stephans, K. Sumorok, M. Varma, D. Velicanu, J. Veverka, J. Wang, T. W. Wang, B. Wyslouch, M. Yang, V. Zhukova

University of Minnesota, Minneapolis, USA
B. Dahmes, A. Evans, A. Finkel, A. Gude, P. Hansen, S. Kalafut, S. C. Kao, K. Klapoetke, Y. Kubota, Z. Lesko, J. Mans, S. Nourbakhsh, N. Ruckstuhl, R. Rusack, N. Tambe, J. Turkewitz

University of Mississippi, Oxford, USA
J. G. Acosta, S. Oliveros

University of Nebraska-Lincoln, Lincoln, USA
E. Avdeeva, K. Bloom, S. Bose, D. R. Claes, A. Dominguez, C. Fangmeier, R. Gonzalez Suarez, R. Kamalieddin, J. Keller, D. Knowlton, I. Kravchenko, F. Meier, J. Monroy, F. Ratnikov, J. E. Siado, G. R. Snow

State University of New York at Buffalo, Buffalo, USA
M. Alyari, J. Dolen, J. George, A. Godshalk, C. Harrington, I. Iashvili, J. Kaisen, A. Kharchilava, A. Kumar, S. Rappoccio, B. Roozbahani

Northeastern University, Boston, USA
G. Alverson, E. Barberis, D. Baumgartel, M. Chasco, A. Hortiangtham, A. Massironi, D. M. Morse, D. Nash, T. Orimoto, R. Teixeira De Lima, D. Trocino, R.-J. Wang, D. Wood, J. Zhang

Northwestern University, Evanston, USA
K. A. Hahn, A. Kubik, N. Mucia, N. Odell, B. Pollack, A. Pozdnyakov, M. Schmitt, S. Stoynev, K. Sung, M. Trovato, M. Velasco

University of Notre Dame, Notre Dame, USA
A. Brinkerhoff, N. Dev, M. Hildreth, C. Jessop, D. J. Karmgard, N. Kellams, K. Lannon, S. Lynch, N. Marinelli, F. Meng, C. Mueller, Y. Musienko[37], T. Pearson, M. Planer, A. Reinsvold, R. Ruchti, G. Smith, S. Taroni, N. Valls, M. Wayne, M. Wolf, A. Woodard

The Ohio State University, Columbus, USA
L. Antonelli, J. Brinson, B. Bylsma, L. S. Durkin, S. Flowers, A. Hart, C. Hill, R. Hughes, W. Ji, K. Kotov, T. Y. Ling, B. Liu, W. Luo, D. Puigh, M. Rodenburg, B. L. Winer, H. W. Wulsin

Princeton University, Princeton, USA
O. Driga, P. Elmer, J. Hardenbrook, P. Hebda, S. A. Koay, P. Lujan, D. Marlow, T. Medvedeva, M. Mooney, J. Olsen, C. Palmer, P. Piroué, H. Saka, D. Stickland, C. Tully, A. Zuranski

University of Puerto Rico, Mayaguez, USA
S. Malik

Purdue University, West Lafayette, USA
V. E. Barnes, D. Benedetti, D. Bortoletto, L. Gutay, M. K. Jha, M. Jones, K. Jung, D. H. Miller, N. Neumeister, B. C. Radburn-Smith, X. Shi, I. Shipsey, D. Silvers, J. Sun, A. Svyatkovskiy, F. Wang, W. Xie, L. Xu

Purdue University Calumet, Hammond, USA
N. Parashar, J. Stupak

Rice University, Houston, USA
A. Adair, B. Akgun, Z. Chen, K. M. Ecklund, F. J. M. Geurts, M. Guilbaud, W. Li, B. Michlin, M. Northup, B. P. Padley, R. Redjimi, J. Roberts, J. Rorie, Z. Tu, J. Zabel

University of Rochester, Rochester, USA
B. Betchart, A. Bodek, P. de Barbaro, R. Demina, Y. Eshaq, T. Ferbel, M. Galanti, A. Garcia-Bellido, J. Han, A. Harel, O. Hindrichs, A. Khukhunaishvili, G. Petrillo, P. Tan, M. Verzetti

Rutgers, The State University of New Jersey, Piscataway, USA
S. Arora, A. Barker, J. P. Chou, C. Contreras-Campana, E. Contreras-Campana, D. Duggan, D. Ferencek, Y. Gershtein, R. Gray, E. Halkiadakis, D. Hidas, E. Hughes, S. Kaplan, R. Kunnawalkam Elayavalli, A. Lath, K. Nash, S. Panwalkar, M. Park, S. Salur, S. Schnetzer, D. Sheffield, S. Somalwar, R. Stone, S. Thomas, P. Thomassen, M. Walker

University of Tennessee, Knoxville, USA
M. Foerster, G. Riley, K. Rose, S. Spanier, A. York

Texas A&M University, College Station, USA
O. Bouhali[67], A. Castaneda Hernandez[67], M. Dalchenko, M. De Mattia, A. Delgado, S. Dildick, R. Eusebi, J. Gilmore,

T. Kamon[68], V. Krutelyov, R. Mueller, I. Osipenkov, Y. Pakhotin, R. Patel, A. Perloff, A. Rose, A. Safonov, A. Tatarinov, K. A. Ulmer[2]

Texas Tech University, Lubbock, USA
N. Akchurin, C. Cowden, J. Damgov, C. Dragoiu, P. R. Dudero, J. Faulkner, S. Kunori, K. Lamichhane, S. W. Lee, T. Libeiro, S. Undleeb, I. Volobouev

Vanderbilt University, Nashville, USA
E. Appelt, A. G. Delannoy, S. Greene, A. Gurrola, R. Janjam, W. Johns, C. Maguire, Y. Mao, A. Melo, H. Ni, P. Sheldon, B. Snook, S. Tuo, J. Velkovska, Q. Xu

University of Virginia, Charlottesville, USA
M. W. Arenton, B. Cox, B. Francis, J. Goodell, R. Hirosky, A. Ledovskoy, H. Li, C. Lin, C. Neu, T Sinthuprasith, X. Sun, Y. Wang, E. Wolfe, J. Wood, F. Xia

Wayne State University, Detroit, USA
C. Clarke, R. Harr, P. E. Karchin, C. Kottachchi Kankanamge Don, P. Lamichhane, J. Sturdy

University of Wisconsin-Madison, Madison, WI, USA
D. A. Belknap, D. Carlsmith, M. Cepeda, S. Dasu, L. Dodd, S. Duric, B. Gomber, M. Grothe, R. Hall-Wilton, M. Herndon, A. Hervé, P. Klabbers, A. Lanaro, A. Levine, K. Long, R. Loveless, A. Mohapatra, I. Ojalvo, T. Perry, G. A. Pierro, G. Polese, T. Ruggles, T. Sarangi, A. Savin, A. Sharma, N. Smith, W. H. Smith, D. Taylor, N. Woods

[†] **Deceased**

1: Also at Vienna University of Technology, Vienna, Austria
2: Also at CERN, European Organization for Nuclear Research, Geneva, Switzerland
3: Also at State Key Laboratory of Nuclear Physics and Technology, Peking University, Beijing, China
4: Also at Institut Pluridisciplinaire Hubert Curien, Université de Strasbourg, Université de Haute Alsace Mulhouse, CNRS/IN2P3, Strasbourg, France
5: Also at National Institute of Chemical Physics and Biophysics, Tallinn, Estonia
6: Also at Skobeltsyn Institute of Nuclear Physics, Lomonosov Moscow State University, Moscow, Russia
7: Also at Universidade Estadual de Campinas, Campinas, Brazil
8: Also at Centre National de la Recherche Scientifique (CNRS)-IN2P3, Paris, France
9: Also at Laboratoire Leprince-Ringuet, Ecole Polytechnique, IN2P3-CNRS, Palaiseau, France
10: Also at Joint Institute for Nuclear Research, Dubna, Russia
11: Now at Suez University, Suez, Egypt
12: Now at British University in Egypt, Cairo, Egypt
13: Also at Cairo University, Cairo, Egypt
14: Also at Fayoum University, El-Fayoum, Egypt
15: Also at Université de Haute Alsace, Mulhouse, France
16: Also at Tbilisi State University, Tbilisi, Georgia
17: Also at RWTH Aachen University, III. Physikalisches Institut A, Aachen, Germany
18: Also at Indian Institute of Science Education and Research, Bhopal, India
19: Also at University of Hamburg, Hamburg, Germany
20: Also at Brandenburg University of Technology, Cottbus, Germany
21: Also at Institute of Nuclear Research ATOMKI, Debrecen, Hungary
22: Also at Eötvös Loránd University, Budapest, Hungary
23: Also at University of Debrecen, Debrecen, Hungary
24: Also at Wigner Research Centre for Physics, Budapest, Hungary
25: Also at University of Visva-Bharati, Santiniketan, India
26: Now at King Abdulaziz University, Jeddah, Saudi Arabia
27: Also at University of Ruhuna, Matara, Sri Lanka
28: Also at Isfahan University of Technology, Isfahan, Iran
29: Also at University of Tehran, Department of Engineering Science, Tehran, Iran
30: Also at Plasma Physics Research Center, Science and Research Branch, Islamic Azad University, Tehran, Iran

31: Also at Università degli Studi di Siena, Siena, Italy
32: Also at Purdue University, West Lafayette, USA
33: Also at International Islamic University of Malaysia, Kuala Lumpur, Malaysia
34: Also at Malaysian Nuclear Agency, MOSTI, Kajang, Malaysia
35: Also at Consejo Nacional de Ciencia y Tecnología, Mexico city, Mexico
36: Also at Warsaw University of Technology, Institute of Electronic Systems, Warsaw, Poland
37: Also at Institute for Nuclear Research, Moscow, Russia
38: Now at National Research Nuclear University 'Moscow Engineering Physics Institute' (MEPhI), Moscow, Russia
39: Also at St. Petersburg State Polytechnical University, St. Petersburg, Russia
40: Also at California Institute of Technology, Pasadena, USA
41: Also at Faculty of Physics, University of Belgrade, Belgrade, Serbia
42: Also at National Technical University of Athens, Athens, Greece
43: Also at Scuola Normale e Sezione dell'INFN, Pisa, Italy
44: Also at National and Kapodistrian University of Athens, Athens, Greece
45: Also at Institute for Theoretical and Experimental Physics, Moscow, Russia
46: Also at Albert Einstein Center for Fundamental Physics, Bern, Switzerland
47: Also at Gaziosmanpasa University, Tokat, Turkey
48: Also at Adiyaman University, Adiyaman, Turkey
49: Also at Mersin University, Mersin, Turkey
50: Also at Cag University, Mersin, Turkey
51: Also at Piri Reis University, Istanbul, Turkey
52: Also at Ozyegin University, Istanbul, Turkey
53: Also at Izmir Institute of Technology, Izmir, Turkey
54: Also at Marmara University, Istanbul, Turkey
55: Also at Kafkas University, Kars, Turkey
56: Also at Mimar Sinan University, Istanbul, Istanbul, Turkey
57: Also at Yildiz Technical University, Istanbul, Turkey
58: Also at Hacettepe University, Ankara, Turkey
59: Also at Rutherford Appleton Laboratory, Didcot, UK
60: Also at School of Physics and Astronomy, University of Southampton, Southampton, UK
61: Also at Instituto de Astrofísica de Canarias, La Laguna, Spain
62: Also at Utah Valley University, Orem, USA
63: Also at University of Belgrade, Faculty of Physics and Vinca Institute of Nuclear Sciences, Belgrade, Serbia
64: Also at Facoltà Ingegneria, Università di Roma, Rome, Italy
65: Also at Argonne National Laboratory, Argonne, USA
66: Also at Erzincan University, Erzincan, Turkey
67: Also at Texas A&M University at Qatar, Doha, Qatar
68: Also at Kyungpook National University, Daegu, Korea